Identification of the manipulator stiffness model parameters in industrial environment

Alexandr Klimchik, Benoit Furet, Stéphane Caro, Anatol Pashkevich

Identification of the manipulator stiffness model parameters in industrial environment

Alexandr Klimchik [a,b],[1] Benoit Furet [b,c], Stéphane Caro [b.d], Anatol Pashkevich [a,b]

[a] *Ecole des Mines de Nantes, 4 rue Alfred-Kastler, Nantes 44307, France*

[b] *Institut de Recherches en Communications et en Cybernétique de Nantes, UMR CNRS 6597, 1 rue de la Noe, 44321 Nantes, France*

[c] *University of Nantes, Chemin de la Censive du Tertre, 44300 Nantes, France*

[d] *Centre National de la Recherche Scientifique (CNRS), France*

Abstract

The paper addresses a problem of robotic manipulator calibration in real industrial environment. The main contributions are in the area of the elastostatic parameters identification In contrast to other works the considered approach takes into account elastic properties of both links and joint. Particular attention is paid to the practical identifiability of the model parameters, which completely differs from the theoretical one that relies on the rank of the observation matrix only, without taking into account essential differences in the model parameter magnitudes and the measurement noise impact. This problem is relatively new in robotics and essentially differs from that arising in geometrical calibration. To solve the problem, physical algebraic and statistical model reduction methods are proposed. They are based on the stiffness matrix sparseness taking into account the physical properties of the manipulator elements, stricture of the observation matrix and also on the heuristic selection of the practically non-identifiable parameters that employs numerical analyses of the parameter estimates. In spite of the fact that main theoretical results have been developed for elastostatic calibration, they can be also efficiently applied for geometric case. The advantages of the developed approach are illustrated by two application examples that deal with elastostatic and geometric calibration of industrial robot in real industrial environment.

Keywords:

Robot calibration, elastostatic identification, stiffness modeling, parameter identifiability, parameter-to-noise ratio

1 Introduction

Industrial robots are gradually finding their niche in manufacturing, replacing less universal and more expensive CNC-machines. Application area of robots is constantly growing, they begin to be used not only for the assembly and pick-and-place operations, but also for the machining. The latter requires special attention to the accuracy of the model, which is used to control the manipulator movements. Furthermore, for this process, the robot is usually subject to essential external loading caused by the machining force that may lead to non-negligible deflections of the end-effector [1] and accordingly degrade the quality of the final product. This issue becomes extremely important in the aerospace industry, where the accuracy requirements are very high but the materials are hard to process. In this case, the manipulator stiffness modelling and corresponding error compensation technique are the key points [2-5], where in addition to accurate geometric model a sophisticated elastostatic one is required.

In practice, the robot positioning accuracy can be improved by means of either on-line or off-line error compensation techniques [6-8]. It is clear that both approaches should rely on the accurate model, which is able to describe the end-effector deviation due to manufacturing tolerances and the external loading. Usually main geometric errors (such as offsets and link lengths) can be efficiently compensated by modifying internal parameters of the robot controller [9, 10]. In contrast, the compliance errors (as well as some geometric errors) have to be compensated via modification of the controller inputs. Relevant on-line compensation strategy requires external measurement system that continuously provides the end-effector coordinates, which are compared with the computed ones (obtained from direct geometric model of the robot controller) and the differences are used for adjusting the input trajectory [11, 12]. The most essential advantage of such an approach is ability to compensate all sources of robot inaccuracy. However, suitable measurement systems are quite expensive and often cannot ensure tracking the reference point in a whole robot workspace. Moreover, behavior of some technological processes hampers the end-effector observability (cutting chip in milling, for instance) and may damage the measurement equipment. In such a case, an off-line error compensation technique looks more reasonable; it is aimed at adjusting the target trajectory in accordance with the errors to be

[1] Corresponding author. Tel. +33 251 85 83 17; fax. +33 251 85 83 49; E-mail address: alexandr.klimchik@mines-nantes.fr (A. Klimchik).

compensated and the geometric model used in the robot controller [7, 13]. It is evident that the efficiency of the latter approach is quite sensitive to the model completeness and the accuracy of its parameters.

To achieve desired degree of accuracy, the manipulator model should be calibrated for each particular [14, 15]. In modern robotics, there exist a number of techniques that allow user to identify geometric and elastostatic parameters of either serial or parallel manipulators. In general, classical calibration procedure contains four basic steps: modeling, measurement, identification and implementation [16]. The first step is aimed at development of a model, which is accurate enough and also is suitable for the identification (i.e. without redundant parameters that can cause numerical problems). Relevant techniques are usually based on different parameterization methods of robot geometry that produce obviously complete (but redundant) models that are subject to further reduction. In early works of Hollerbach [17], Veitschegger and Wu [18], the Denavit-Hartenberg (D-H) parameterization was used, which describes the link-to-link transformations via 4 geometric parameters only that does not guaranty the model completeness in general case. Later, Hollerbach et. al. [19] and Hayati et. al. [20, 21] modified the D-H approach by utilizing 5 parameters to describe these transformations. Further developments led to models with 6 parameters per transformation, they have been used by Stone [22] and Whintey et. al. [23]. Any of these parameterizations can be used for geometric modeling; however to be suitable for calibration, the number of the parameters should be non-redundant. In practice, the maximum number of the identifiable geometric parameters is evaluated using so-called POE formula [24, 25].

In the manipulator stiffness modelling, there are three main approaches: the Finite Element Analysis (FEA), the Matrix Structural Analysis (MSA), and the Virtual Joint Method (VJM). The most accurate of them is the FEA-based technique [26], which allows presenting manipulator components with their true shape and dimension. However, this method is usually applied at the final design stage because of the high computational expenses [27]. The MSA method [28] incorporates the main ideas of the FEA, but operates with rather large elements – 3D flexible beams. This obviously leads to the reduction of the computational efforts, but does not eliminate the disadvantages of FEA. And finally, the VJM method [29-32], is based on the extension of the traditional rigid model by adding the virtual joints (localized springs), which describe the elastic deformations of the links, joints and actuators. This technique provides reasonable trade-off between the model accuracy and computational complexity, which will be further used in this paper.

At the following step, the measurement data are obtained that are required for the identification equations. These data can be gotten using open-loop and closed-loop methods. The first approach provides the Cartesian coordinates of the reference point(s) using external measurement system (laser tracker or coordinate measurement machine, for instance). The second approach uses some physical constraints imposed on the end-effector (by fixing the reference point or assuming that it belongs to a plane, for instance) that create an auxiliary closed-loop providing the desired measurement data. In practice, both approaches are used. For example, Nubiola and Bonev [33], Bai et. al. [34], and Klimchik et. al. [35] used the laser tracker systems for geometric and elastostatic calibrations. An alternative technique was used by Takeda et. al. [36] who utilized the double ball-bar system for calibration in-parallel actuated mechanisms. The end-effector plane constraints were used by Ikits and Hollerbach [37] to calibrate a serial anthropomorphic manipulator.

The next step, identification, is aimed at tuning the model parameters in accordance with the experimental data. It should be mentioned that in the literature there exist different algorithms to solve this problem, which differ in the type of original measurement data (Cartesian coordinates, distance to the reference point/line, end-effector orientation, etc.) and numerical optimization techniques (gradient search, simulated annealing, genetic algorithms, etc.). Some of them are implemented in ROSY software [38], which can be applied for calibration of both serial and parallel robots using measuring tool with two digital CCD cameras. An alternative geometric parameter identification method that is based on a laser-ranger attached to the end-effector was used in [39]. In [40], dedicated differential techniques were applied that use measurement data from structured laser module and stationary camera in order to estimate parameters of 7-DOF humanoid manipulator arm. In [41], the authors applied a backpropagation neural network to compensate the joint errors of the neurosurgical robot system. Santolaria et.al. [42] utilised the ball bar gauge measurement device and identification technique whose objective function includes terms that are regarding repeatability and measurement accuracy. To improve the static positioning accuracy of the PA10-6CE robot, in [43] a 30-parameter model incorporating elastostatic ones has been used. The screw measurement method that utilizes laser tracker with an active target and identification procedure that is based on circle point analysis was used in [44] to identify the kinematic parameters of an industrial robot. In [45], the authors presented a 12-parameter error kinematic model for the three linear actuators of the Gantry-Tau robot and used three types of measurement equipments (laser interferometers, linear encoders and double-ball bars) to calibrate the linear actuators.

The last step, implementation, deals with modification the robot control software in accordance with the parameters identified at the previous step. However, in practice, commercial robot software is not opened and rather limited number of manipulator parameters can be modified directly (to simplify direct and inverse kinematics, it is usually assumed that a number of joint axis are strictly parallel or orthogonal). For this reason, the most common technique is the modification of the robot control program (i.e. adjusting of the robot control inputs related to the target trajectory), which can be also treated as the compensation of the

difference between nominal and real parameters identified from the experimental study . On this level it is not supposed to use any additional measurement equipment (in contrast to general compensation strategies described above). To compensate manipulator positioning errors, both on-line and off-line methods can be applied. The simplest approach here is so-called the "mirror" technique that has been applied in [7, 46] to compensate the compliance errors. The modification of this method proposed by Klimchik et. al. [4, 13] is able to take into account non-linear properties of the geometric and elastostatic model.

To improve identification accuracy, it is possible to include an additional step into the calibration procedure that is aimed at selection of optimal measurement configurations (it can be treated as design of calibration experiments). This idea has been used by a number of authors and allowed them to reduce calibration errors without increasing the cost of experiments. In particular, Borm and Menq [47] showed that proper selection of measurement configurations is more important for the identification accuracy than simply increasing the number of measurements m that yields the improvement factor $1/\sqrt{m}$ [48]. It should be mentioned that even for fully automated measurement systems [49, 50] where the cost of each experiment is relatively low, this issue remains important because it is more efficient if the measurement configurations are selected properly. For this reason, there are a number of works devoted to the optimal measurement configurations selection that are based on different criterion and employ some techniques known from the classical design of experiment theory [48]. For example, Khalil et. al. [51] determined the set of optimal measurement configurations by minimizing the condition number of the observation matrix. Nahvi and J. M. Hollerbach [52] used the noise amplification index to find the measurement configurations. Daney [53] used the constrained optimization algorithm based on the minimization of the singular values product for Gough platform calibration. In [54], the idea from D-optimality criteria has been used to quantify optimal measurement configurations for a general nR planar manipulators. Zhuang et. al. [55] applied simulating annealing to find measuring configurations that are optimal with respect to two considered performance measures. In some works, to qualify sets of measurement configurations, the robot positioning accuracy after calibration has been used as a performance index [56, 57].

It should be mentioned that calibration of the elasto-static model is much more difficult compared to the geometric one. For a simple case, when only elasticity of the actuated joints is taken into account, an efficient approach has been proposed in [58, 59], but this simplification does not allow describing some important deflections of the end-effector. More sophisticated model describing both the joint and link elasticity can be developed use CAD-based technique proposed in our previous work [60]. However, this model includes huge number of parameters that cannot be identified separately using conventional measurement data (describing end-effector deflections caused by external force/torque). It means that from mathematical point of view, this technique may produce redundant models that are not suitable for calibration. For instance, attempts to solve the identification problem for the whole set of the elastostatic parameters (258 for 6 d.o.f. manipulator) leads to the fail of the numerical routines that is caused by singularity of the relevant observation matrix.

As follows from literature review, similar problem is also known in geometric calibration where the concept of *complete-irreducible-continues* model has been introduced and relevant algebraical tools for the model reduction have been developed [61-63]. However, in elastostatic calibration there is an additional difficulty caused by high number of relatively small parameters for which the measurement noise impact is very essential. According to our experience, even for non-redundant models, the identification results may violate fundamental physical properties of the stiffness matrices, such as *positive-definiteness and symmetry*, and are not acceptable for the compliance error compensation (more details are given in Section 3.2 presenting a motivation example). For this reason, this paper introduces a new notion of *practical identifiability* and proposes corresponding model reduction methods that allow obtaining reliable results in real industrial environment.

To address the above mentioned problem, the remainder of the paper is organised as follows. Section 2 presents the stiffness modelling background. Section 3 describes the elastostatic calibration procedure and contains a motivation example allowing us to define the research problems. In Section 4, the developed model reduction methods are presented. Section 5 contains application examples that illustrate advantages of the proposed technique. And finally, Section 6 summarises the main contributions of the paper.

2 Manipulator stiffness modeling background

Let us consider elastostatic model of a general serial manipulator, which consists of a fixed "Base", a serial chain of flexible "Links", a number of flexible actuated joints "Ac" and an "End-effector" (Figure 1). It is assumed that all links are separated by either rotational or translational joints. Such architecture can be found most of industrial serial robots.

In order to evaluate the stiffness of the considered manipulator, let us apply the virtual joint method (VJM), which is based on the lump modelling approach [64, 65]. According to this approach, the original rigid model should be extended by adding virtual joints (localized springs), which describe elastic deformations of the links. Besides, virtual springs are included in the actuated joints, in order to take into account the stiffness of the control loop. Under these assumptions, the kinematic chain can be described by the following serial structure:

(a) a rigid link between the manipulator base and the first actuated joint described by the constant homogenous transformation matrix $\mathbf{T}_{\text{Base}}$;

(b) several flexible actuated joints described by the homogeneous matrix function $\mathbf{T}^i_{\text{Joint}}(q^i + \theta^i_{\text{Ac}})$, which depends on the actuated joint variable q^i and the virtual joint variable θ^i_{Ac} that takes into account the joint compliance;

(c) a set of rigid links, which are described by the constant homogenous transformation matrices $\mathbf{T}^i_{\text{Link}}$;

(d) a set of 6-d.o.f. virtual joints that take into account the link flexibility and are described by the homogeneous matrix function $\mathbf{T}_{\text{VJM}}(\boldsymbol{\theta}^i_{\text{Link}})$ which depends on the virtual joint variables $\boldsymbol{\theta}^i_{\text{Link}} = (\theta^i_{\text{x}}, \theta^i_{\text{y}}, \theta^i_{\text{z}}, \theta^i_{\varphi\text{x}}, \theta^i_{\varphi\text{y}}, \theta^i_{\varphi\text{z}})$ corresponding to the translation/rotation deflexions in/around the axis x, y, z;

(e) a rigid link from the last joint to the end-effector, described by the constant homogenous matrix transformation $\mathbf{T}_{\text{Tool}}$.

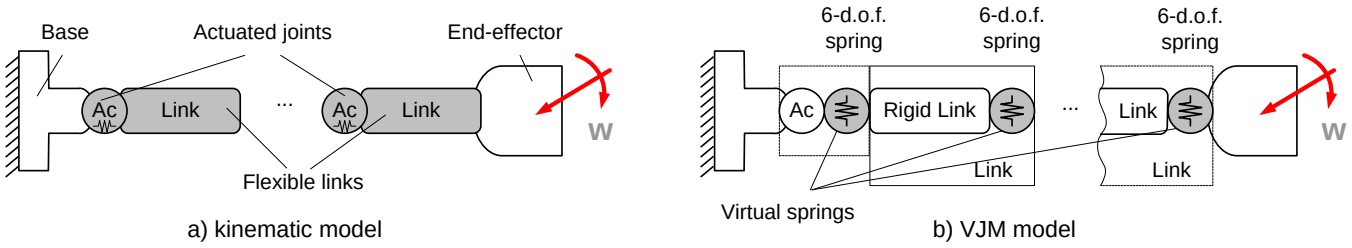

Figure 1 Serial manipulator and its VJM model

In the frame of these notations, the final expression defining the end-effector location subject to variations of all joint coordinates may be presented as the product of the following homogenous matrices and matrix functions

$$\mathbf{T} = \mathbf{T}_{\text{Base}} \cdot \left[\prod_{i=1}^{n} \mathbf{T}^i_{\text{Joint}}(q^i + \theta^i_{\text{Ac}}) \cdot \mathbf{T}^i_{\text{Link}} \cdot \mathbf{T}_{\text{VJM}}\left(\boldsymbol{\theta}^i_{\text{Link}}\right) \right] \cdot \mathbf{T}_{\text{Tool}} \tag{1}$$

where n is the number of links/joints, and the components $\mathbf{T}_{\text{Base}}$, , $\mathbf{T}^i_{\text{Joint}}(.)$, $\mathbf{T}^i_{\text{Link}}$, $\mathbf{T}_{\text{VJM}}(.)$, $\mathbf{T}_{\text{Tool}}$ may be factorized with respect to the terms including the joint variables (in order to simplify computing of the derivatives). For further convenience, after extraction from the homogeneous matrix $\mathbf{T}$ rotation and translation components [66], the kinematic model can be rewritten in more conventional form

$$\mathbf{t} = \mathbf{g}(\mathbf{q}, \boldsymbol{\theta}) \tag{2}$$

where $\mathbf{g}(.)$ denotes relevant vector function, the vector $\mathbf{t} = (\mathbf{p}, \boldsymbol{\varphi})^{\text{T}}$ defines the end-effector position $\mathbf{p} = (x, y, z)^{\text{T}}$ and orientation $\boldsymbol{\varphi} = (\varphi_{\text{x}}, \varphi_{\text{y}}, \varphi_{\text{z}})^{\text{T}}$, the vector $\mathbf{q} = (q_1, q_2, ..., q_{\text{n}})^{\text{T}}$ aggregates all actuated coordinates, the vector $\boldsymbol{\theta} = (\theta_1, \theta_2, ..., \theta_{\text{n}\theta})^{\text{T}}$ collects all virtual joint coordinates, and n_θ is the number of the virtual joints. It should be noted that here the values of coordinates $\mathbf{q}$ are completely defined by the robot controller, while the values of the virtual joint coordinates $\boldsymbol{\theta}$ depend on the external loading applied to the robot end-effector.

To take into account manipulator stiffness properties, let us assume that variations in the virtual joint variables $\boldsymbol{\theta}$ generate the force/torque applied to the corresponding links that are evaluated by the following linear equation (it can be treated as a generalised Hooke's law for the manipulator) $\boldsymbol{\tau}_\theta = \mathbf{K}_\theta \cdot \boldsymbol{\theta}$, where $\boldsymbol{\tau}_\theta = (\tau_{\theta,1}, \tau_{\theta,2}, ..., \tau_{\theta,\text{n}\theta})^{\text{T}}$ is the aggregated vector of the virtual joint reactions, $\mathbf{K}_\theta = diag(\mathbf{K}_{\theta,1}, \mathbf{K}_{\theta,2}, ..., \mathbf{K}_{\theta,\text{n}\theta})$ is the aggregated virtual spring stiffness matrix, and $\mathbf{K}_{\theta,i}$ is the spring stiffness matrix of the corresponding link/joint. Further, let us apply the principle of virtual work assuming that the joints are given small, arbitrary virtual displacements $\Delta\boldsymbol{\theta}$ in the equilibrium neighbourhood. Then, the virtual work of the external wrench $\mathbf{w}$ applied to the end-effector along the corresponding displacement $\Delta\mathbf{t} = \mathbf{J}_\theta \cdot \Delta\boldsymbol{\theta}$ is equal to $(\mathbf{w}^{\text{T}} \cdot \mathbf{J}_\theta) \cdot \Delta\boldsymbol{\theta}$, where $\mathbf{J}_\theta = \partial f(\mathbf{q}, \boldsymbol{\theta}) / \partial\boldsymbol{\theta}$ is the kinematic Jacobians with respect to the virtual variables $\boldsymbol{\theta}$, which may be computed from (2) analytically or semi-analytically, using the factorization technique proposed in [64]. On the other hand, for the internal forces $\boldsymbol{\tau}_\theta$, the virtual work includes only one component $-\boldsymbol{\tau}_\theta{}^{\text{T}} \cdot \Delta\boldsymbol{\theta}$. Therefore, since in the static equilibrium the total virtual work is equal to zero for any virtual displacement, the equilibrium conditions may be written as

$$\mathbf{J}_\theta{}^{\text{T}} \cdot \mathbf{w} = \boldsymbol{\tau}_\theta \tag{3}$$

This gives additional expressions describing the force/torque propagation from the joints to the end-effector that should be considered simultaneously with the geometric equation (2).

Combining further the virtual joint reaction equation $\boldsymbol{\tau}_\theta = \mathbf{K}_\theta \cdot \boldsymbol{\theta}$, the equilibrium condition (3) and the linearized geometric model $\Delta\mathbf{t} = \mathbf{J}_\theta \cdot \Delta\boldsymbol{\theta}$, it is possible to write statics equations

$$\mathbf{J}_\theta \cdot \boldsymbol{\theta} = \Delta\mathbf{t}; \qquad \mathbf{w} \cdot \mathbf{J}_\theta{}^{\mathrm{T}} - \mathbf{K}_\theta \cdot \boldsymbol{\theta} = 0 \tag{4}$$

describing elastostatic properties of the considered manipulator. In these equations, the end-effector displacement $\Delta\mathbf{t}$ is treated as the model input and the external wrench $\mathbf{w}$ is the model output, which corresponds to the representation of the manipulator stiffness matrix in the following form

$$\mathbf{W} = \mathbf{K}_C \cdot \Delta\mathbf{t} \tag{5}$$

where $\mathbf{K}_C$ is the desired Cartesian stiffness matrix of the considered manipulator for given robot configuration $\mathbf{q}$. To find this matrix, equations (4) may be presented in the matrix form

$$\begin{bmatrix} \mathbf{0} & \mathbf{J}_\theta \\ \mathbf{J}_\theta{}^{\mathrm{T}} & -\mathbf{K}_\theta \end{bmatrix} \cdot \begin{bmatrix} \mathbf{w} \\ \boldsymbol{\theta} \end{bmatrix} = \begin{bmatrix} \Delta\mathbf{t} \\ \mathbf{0} \end{bmatrix} \tag{6}$$

and solved for $\mathbf{W}$. This transformation yields the following force-deflection relation $\mathbf{J}_\theta \cdot \mathbf{K}_\theta^{-1} \cdot \mathbf{J}_\theta{}^{\mathrm{T}} \cdot \mathbf{w} = \Delta\mathbf{t}$ that allows us to express the manipulator Cartesian stiffness matrix as

$$\mathbf{K}_C = \left(\mathbf{J}_\theta \cdot \mathbf{K}_\theta^{-1} \cdot \mathbf{J}_\theta{}^{\mathrm{T}} \right)^{-1} \tag{7}$$

This expression allows us to compute the Cartesian stiffness matrix assuming that the matrix $\mathbf{K}_\theta = diag(\mathbf{K}_\theta^{(1)}, \mathbf{K}_\theta^{(2)}, ...)$, defining elastostatic properties of the manipulator links/joins is given. However, in practice, the matrices $\left\{\mathbf{K}_\theta^{(i)}, i = 1, 2, ...\right\}$ are unknown and should be identified from relevant experiments. However, there are a number of numerical problems that may arise here that are in the focus of the remaining parts of the paper.

3 Problem of elastostatic parameters identification

3.1 Methodology of elastostatic identification

To estimate the desired matrices describing elasticity of the manipulator components (i.e., compliances of the virtual springs presented in Fig. 1), the elastostatic model (5) should be rewritten as

$$\Delta\mathbf{t} = \sum\nolimits_{i=1}^{n} \left(\mathbf{J}_\theta^{(\mathrm{i})} \mathbf{k}_\theta^{(\mathrm{i})} \mathbf{J}_\theta^{(\mathrm{i})\mathrm{T}} \right) \cdot \mathbf{w} \tag{8}$$

where $\Delta\mathbf{t}$ is the vector of the end-effector displacements under the loading $\mathbf{w}$, the matrices $\mathbf{k}_\theta^{(\mathrm{i})} = (\mathbf{K}_\theta^{(\mathrm{i})})^{-1}$ denote the link/joint compliances that should be identified via calibration, and the matrices $\mathbf{J}_\theta^{(\mathrm{i})}$ are corresponding sub-Jacobians obtained by the fractioning of the aggregated Jacobian $\mathbf{J}_\theta^T = [\mathbf{J}_\theta^{(1)^T}, \mathbf{J}_\theta^{(2)^T}, ...]$. For the identification purposes, this expression should be transformed into more convenient form, where all desired parameters (elements of the matrices $\mathbf{k}_\theta^{(\mathrm{i})}, i = 1, 2, ...$) are collected in a single vector $\boldsymbol{\pi} = (k_{\theta 11}^{(1)}, k_{\theta 12}^{(1)}, ... k_{\theta 66}^{(n)})$. It yields the following linear equation

$$\Delta\mathbf{t} = \mathbf{A}(\mathbf{q}, \mathbf{w} \mid \boldsymbol{\pi}) \cdot \boldsymbol{\pi} \tag{9}$$

where

$$\mathbf{A}(\mathbf{q}, \mathbf{w} \mid \boldsymbol{\pi}) = [\mathbf{J}_1 \mathbf{J}_1^T \mathbf{w}, \mathbf{J}_2 \mathbf{J}_2^T \mathbf{w}, ..., \mathbf{J}_m \mathbf{J}_m^T \mathbf{w}] \tag{10}$$

is so-called observation matrix that defines the mapping between the unknown compliances $\boldsymbol{\pi}$ and the end-effector displacements $\Delta\mathbf{t}$ under the loading $\mathbf{w}$ for the manipulator configuration $\mathbf{q}$. Below, for the presentation convenience this matrix will be also referred to as $\mathbf{A}_\pi$, where the subscript defines the parameters set for which the observation matrix is computed. Here, the vectors $\mathbf{J}_i$ are the columns of the matrix $\mathbf{J}_\theta$, i.e. $\mathbf{J}_\theta = [\mathbf{J}_1, \mathbf{J}_2, ..., \mathbf{J}_m]$.

Taking into account that the calibration experiments are carried out for several manipulator configurations defined by the actuated joint coordinates $\mathbf{q}_j$, $j = \overline{1, m}$, the system of basic equations for the identification can be presented in the following form

$$\Delta\mathbf{t}_j = \mathbf{A}(\mathbf{q}_j, \mathbf{w}_j \mid \boldsymbol{\pi}) \cdot \boldsymbol{\pi} + \boldsymbol{\varepsilon}_j; \qquad j = \overline{1, m} \tag{11}$$

where $\boldsymbol{\varepsilon}_j$ denotes the vector of measurement errors. For further convenience, let us also present the system of m equation (11) in a matrix form

$$\Delta\mathbf{t}_a = \mathbf{A}_a(\mathbf{q}_a, \mathbf{w}_a \mid \boldsymbol{\pi}) \cdot \boldsymbol{\pi} + \boldsymbol{\varepsilon}_a \tag{12}$$

where subscript "a" indicates that matrices/vector aggregate corresponding components for m configurations. Below, the matrix function $\mathbf{A}_a(\mathbf{q}_a, \mathbf{w}_a \mid \boldsymbol{\pi})$ will be also referred to as $\mathbf{A}_a^{\pi}$. Further, using these notations and assigning proper weights for each equation, the identification can be reduced to the following optimization problem

$$F = \sum_{j=1}^{m} (\mathbf{A}_{\pi j}\boldsymbol{\pi} - \Delta\mathbf{t}_j)^T \boldsymbol{\eta}^T \boldsymbol{\eta} (\mathbf{A}_{\pi j}\boldsymbol{\pi} - \Delta\mathbf{t}_j) \to \min_{\boldsymbol{\pi}} \tag{13}$$

where $\boldsymbol{\eta}$ is the matrix of weighting coefficients that normalizes the measurement data, $\mathbf{A}_{\pi j} = \mathbf{A}(\mathbf{q}_j, \mathbf{w}_j \mid \boldsymbol{\pi})$. This minimization problem yields the following solution

$$\hat{\boldsymbol{\pi}} = \left(\sum_{j=1}^{m} \mathbf{A}_{\pi j}^T \boldsymbol{\eta}^T \boldsymbol{\eta} \mathbf{A}_{\pi j} \right)^{-1} \cdot \left(\sum_{j=1}^{m} \mathbf{A}_{\pi j}^T \boldsymbol{\eta}^T \boldsymbol{\eta} \Delta\mathbf{t}_{\pi j} \right). \tag{14}$$

If the measurement noise is Gaussian (as it is assumed in conventional calibration techniques), expression (14) provides us with a unbiased estimates for which $E(\hat{\boldsymbol{\pi}}) = \boldsymbol{\pi}$. Corresponding covariance matrix evaluating the dispersion of the parameter estimate $\hat{\boldsymbol{\pi}}$ from one identification session to another can be computed as follows

$$\mathrm{cov}(\hat{\boldsymbol{\pi}}) = \left(\sum_{j=1}^{m} \mathbf{A}_{\pi j}^T \boldsymbol{\eta}^T \boldsymbol{\eta} \mathbf{A}_{\pi j} \right)^{-1} \sum_{j=1}^{m} \mathbf{A}_{\pi j}^T \boldsymbol{\eta}^T \boldsymbol{\eta} \boldsymbol{\Sigma}^2 \boldsymbol{\eta}^T \boldsymbol{\eta} \mathbf{A}_{\pi j} \left(\sum_{j=1}^{m} \mathbf{A}_{\pi j}^T \boldsymbol{\eta}^T \boldsymbol{\eta} \mathbf{A}_{\pi j} \right)^{-1} \tag{15}$$

where the matrix $\boldsymbol{\Sigma}^2 = E(\boldsymbol{\varepsilon} \cdot \boldsymbol{\varepsilon}^T)$ describes the statistical properties of the measurement errors.

It can be proved [67] that the best results in terms of the identification accuracy are achieved if $\boldsymbol{\eta} = \boldsymbol{\Sigma}^{-1}$. It leads to the following covariance matrix of the manipulator compliance parameters

$$\mathrm{cov}(\hat{\boldsymbol{\pi}}) = \left(\sum_{j=1}^{m} \mathbf{A}_{\pi j}^T \boldsymbol{\Sigma}^{-T} \boldsymbol{\Sigma}^{-1} \mathbf{A}_{\pi j} \right)^{-1} \tag{16}$$

Such assignment of the weighing coefficients $\boldsymbol{\eta}$ also allows us to avoid the problem of different units in the objective function (13), which arises in straightforward application of the leas-square technique to the robot parameters identification if the measurement system provides both position and orientation data. It should be noted that this particularity is usually omitted in conventional robot calibration. Another way to improve the identification accuracy is related to the proper selection of manipulator measurement configurations $\{\mathbf{q}_j,\ j = \overline{1, m}\}$ that is also known as the calibration experiment planning [68], which directly influences on the observation matrices $\mathbf{A}(\mathbf{q}_j, \mathbf{w}_j \mid \boldsymbol{\pi})$ and on the covariance matrix (16).

It is clear that expression (14) gives reliable estimates of the parameters $\boldsymbol{\pi}$ if and only if the matrix $\sum_{j=1}^{m} \mathbf{A}_{\pi j}^T \boldsymbol{\Sigma}^{-T} \boldsymbol{\Sigma}^{-1} \mathbf{A}_{\pi j}$ is invertible. It leads to the problem of the parameter *identifiability* that have been studied by a number of authors for the problem of geometrical calibration [62, 63]. Relevant techniques are based on the *information matrix rank analysis* (via either SVD- or QR-decomposition). However, in real industrial practice where the measurement not is non-negligible, the identifiable parameters are not equivalent in terms of accuracy (both absolute and relative) and expression (14) can give rather surprising results for some of them. This motivates revision of the above mentioned notion (parameter identifiability) and its extension taking into account the identification accuracy defined by the *covariance matrix* (16). In the following sub-sections, the notion of *practical identifiability* is introduced and a motivation example is presented, which illustrates potential problems that may arises in the manipulator elastostatic calibrations if conventional techniques are applied.

3.2 Difficulties in elastic parameters identification

To illustrate the problems that may arise in identification of the manipulator elastostatic parameters, let us consider a numerical example that deals with a single link of the Orthoglide manipulator (Figure 2). Its compliance matrix has been obtained in [64] and is equal to

$$\mathbf{k} = \left[\begin{array}{ccc:ccc} 4.50\cdot10^{-8} & 0 & 0 & 0 & 0 & 0 \\ 0 & 8.01\cdot10^{-5} & 0 & 0 & 0 & 3.98\cdot10^{-4} \\ 0 & 0 & 3.64\cdot10^{-5} & 0 & -1.71\cdot10^{-4} & 0 \\ \hdashline 0 & 0 & 0 & 3.76\cdot10^{-3} & 0 & 0 \\ 0 & 0 & -1.71\cdot10^{-4} & 0 & 1.09\cdot10^{-3} & 0 \\ 0 & 3.98\cdot10^{-4} & 0 & 0 & 0 & 2.65\cdot10^{-3} \end{array}\right] \tag{17}$$

where the values are expressed in SI units (N, m, rad).

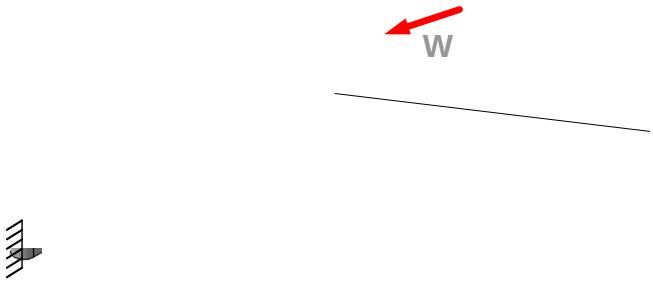

(a) Principal link of Orthoglide manipulator (b) Architecture of Orthoglide manipulator

Figure 2 Manipulator link considered in the motivation example

Let us simulate the calibration process assuming that the matrix (17) should be estimated by means of the identification algorithm described above, where the input data are generated by means of virtual experiments. In the frame of these experiments, the link is assumed to be fixed on one side and the external loading $\mathbf{w}_j$ is applied on the another side. For each loading, the corresponding deflection vector is computed in accordance with expression $\Delta\mathbf{t}_j = \mathbf{k}\cdot\mathbf{w}_j + \boldsymbol{\varepsilon}_j$, where $\boldsymbol{\varepsilon}_j$ is the measurement noise. In accordance with the physical properties of the examined link and to conserve the linearity of the force-deflection relation, the loading magnitude has been limited by $10N$ for the forces and $10Nm$ for the torques. The measurement noise magnitude has been defined as $\sigma_p = 25\mu m$ for the positional components and as $\sigma_\varphi = 0.25 mrad$ for the orientation components (these values correspond to the precision of the best industrial measurement systems that currently are available on the market). These virtual experiments has been carried out six times, in order to obtain sufficient number of equations for the identification of 36 desired parameters k_{ij}.

For these virtual experiments, the properties of the observation matrix used in the identification expression are quite good: rank is equal to 36 and the condition number is 1.00. Nevertheless, the identification are rather "surprising": the obtained compliance matrix essentially differs from the original one and is

$$\hat{\mathbf{k}} = \left[\begin{array}{cccccc} \textit{-3.05·10}^{-8} & -8.71\cdot10^{-8} & 1.86\cdot10^{-7} & 1.59\cdot10^{-7} & -7.72\cdot10^{-8} & 1.15\cdot10^{-7} \\ 4.53\cdot10^{-7} & \textit{8.05·10}^{-5} & -2.07\cdot10^{-7} & 1.98\cdot10^{-7} & 1.14\cdot10^{-7} & \textit{3.98·10}^{-4} \\ 2.29\cdot10^{-7} & 3.76\cdot10^{-7} & \textit{3.65·10}^{-5} & -2.25\cdot10^{-7} & \textit{-1.71·10}^{-4} & 1.13\cdot10^{-7} \\ \hdashline -1.42\cdot10^{-7} & 1.83\cdot10^{-6} & 7.05\cdot10^{-7} & \textit{3.76·10}^{-3} & 1.11\cdot10^{-6} & 4.12\cdot10^{-6} \\ 3.27\cdot10^{-6} & 1.23\cdot10^{-6} & \textit{-1.68·10}^{-4} & 3.99\cdot10^{-6} & \textit{1.09·10}^{-3} & -5.07\cdot10^{-6} \\ -2.61\cdot10^{-6} & \textit{3.97·10}^{-4} & -1.06\cdot10^{-6} & 2.81\cdot10^{-7} & -4.58\cdot10^{-8} & \textit{2.65·10}^{-3} \end{array}\right] \qquad (18)$$

Detailed comparison analysis of the original matrix $\mathbf{k}$ and its estimate $\hat{\mathbf{k}}$ allows us to make the following conclusions concerning the harmful impact of the measurement noise on the identification of the elastostatic parameters in real industrial environment:

(i) the obtained compliance matrix $\hat{\mathbf{k}}$ *may lose the properties of positive-definiteness*, which completely contradicts to the common physical sense that is based on the energy-based definition of $\mathbf{k}^{-1}$ (in particular, in the above example, $\hat{\mathbf{k}}_{11} < 0$ is not acceptable);

(ii) the obtained matrix $\hat{\mathbf{k}}$ *may be non-symmetric*, which also contradicts to the physical sense (for instance, $\hat{\mathbf{k}}_{53}$ and $\hat{\mathbf{k}}_{35}$, which corresponds to non-zero elements of $\mathbf{k}$, are not equal and differ by 2%);

(iii) for some small elements, the *identification accuracy may be extremely low* (for example the element $\hat{\mathbf{k}}_{11}$, which is $\sim 10^3$ times less than $\hat{\mathbf{k}}_{22}$ and $\hat{\mathbf{k}}_{33}$ has been identified completely wrongly);

(iv) in the obtained matrix $\hat{\mathbf{k}}$, the *number of non-zero elements is redundant* compared to the original matrix $\mathbf{k}$; moreover, it is difficult to distinguish small elements $\hat{k}_{ij}$ from so-called zero elements, which correspond to exact zeros in $\mathbf{k}$ induced by the physical properties of the examined link (for instance, the element $\hat{k}_{21}$ that should be equal to zero by definition is the same order of magnitude as $\hat{k}_{11}$, which should be small but strictly positive);

(v) *for the remaining elements*, whose magnitude is high enough, the *identification errors are quite acceptable* (from 0.01% to 1.67%), but they should be further reduced by increasing number of the experiments.

It should be noted that for essentially lower measurement noise (with σ_p and σ_φ that are 100 times smaller) the above mentioned problems do not exist, however such measurement precision is not achievable in industrial environment at present.

Hence, as follows from this motivation example, the whole set of 36 elastostatic parameters $\{k_{ij}\}$ composing the 6×6 matrix $\mathbf{k}$ cannot be estimated using commercially available measurement systems. The main reason for this difficulty is that, for some

elements, corresponding deflections under the admissible loading are comparable with the measurement noise. To detect these indistinct elements, a simple indicator can be applied showing *parameter-to-noise ratio* (which is similar to signal-to-noise ratio in communication):

$$\left[\frac{|\hat{k}_{ij}|}{\sigma_{ij}}\right] = \left[\begin{array}{cccccc} \mathit{0.12} & 0.35 & 0.74 & 0.64 & 0.31 & 0.46 \\ 1.81 & \mathit{322} & 0.83 & 0.79 & 0.46 & \mathit{1593} \\ 0.91 & 1.50 & \mathit{146} & 0.89 & \mathit{684} & 0.45 \\ \hline 0.06 & 0.73 & 0.28 & \mathit{1504} & 0.44 & 1.64 \\ 1.31 & 0.49 & \mathit{-67.3} & 1.60 & \mathit{436} & 2.02 \\ 1.04 & \mathit{159} & 0.42 & 0.11 & 0.02 & \mathit{1060} \end{array}\right] \tag{19}$$

where σ_{ij} is a corresponding element of the relevant covariance matrix. As follows from these numerical values, 27 of 36 desired parameters can be hardly estimated from the experimental data with realistic measurement noise. Only for 9 parameters k_{22}, k_{26}, k_{33}, k_{35}, k_{44}, k_{53}, k_{55}, k_{62}, k_{66} the ratio is high enough (more than 50), so they can be treated as "*practically identifiable*". It should be stressed that similar indicators computed using exact values of k_{ij} (which are unknown in practice) give similar result

$$\left[\frac{|k_{ij}|}{\sigma_{ij}}\right] = \left[\begin{array}{cccccc} 0.18 & 0 & 0 & 0 & 0 & 0 \\ 0 & 320 & 0 & 0 & 0 & 1592 \\ 0 & 0 & 146 & 0 & 684 & 0 \\ \hline 0 & 0 & 0 & 1504 & 0 & 0 \\ 0 & 0 & 68.4 & 0 & 436 & 0 \\ 0 & 159 & 0 & 0 & 0 & 1060 \end{array}\right] \tag{20}$$

allowing us to detect the same set of small or zero parameters whose identifiability is questionable. On the other side, the impact of these parameters on the elastostatic deflections is so small that they can be reasonably excluded from the desired stiffness model. These results confirm importance of the above pointed problems, which below are considered in details.

Summarising theoretical background and simulation results presented above, it is possible to make the following conclusions:

(i) complete elastostatic model of robotic manipulator includes *huge number of parameters* (258 for conventional 6 d.o.f. serial robot), whose simultaneous identification in presence of measurement noise is rather difficult or even impossible;

(ii) before applying the least-square identification technique , the manipulator elastostatic model should be reduced and *redundant parameters* should be eliminated, in order to ensure invertibility of the information matrix; this step can be performed using techniques similar to those developed for the geometrical calibration;

(iii) among the remaining non-redundant parameters, there are a number of non-significant ones, whose absolute values are relatively small, the identification accuracy is quite low and the impact on the compliance of the of the entire manipulator is almost negligible; these parameters can be treated as "*practically non-identifiable*" and should be also eliminated from the model, but relevant techniques are not available yet;

(iv) while developing relevant techniques allowing detection of "*practically identifiable*" *parameters*, it is prudent to take into account some specific properties of the compliance matrices induced by the elasticity physics such as the compliance matrix symmetry, presence of strictly zero elements (matrix sparseness), positive-definiteness, etc.

Hence, to obtain reliable stiffness model that is suitable for calibration, and that contains only significant and practically identifiable parameters while describing manipulator elastostatic properties sufficiently good, it is necessary to develop dedicated model reduction techniques and relevant rules allowing us to minimise number of parameters to be estimated and to reconstruct the original VJM-based model from these data taking into account mathematical relations between the model parameters caused by their physical sense.

4 Practical identifiability in manipulator calibration

4.1 Basic assumptions and terminology

Let us assume that the vector of desired elastostatic parameters $\boldsymbol{\pi}$ should be identified from the set of the linear equations (11) whose least square solution is defined by the expression (14), where the observation matrices $\mathbf{A}(\mathbf{q}_j, \mathbf{w}_j \,|\, \boldsymbol{\pi})$ are computed for certain set of measurement configurations $\{\mathbf{q}_j\}$ and loadings $\{\mathbf{w}_j\}$. Depending on the matrix set $\{\mathbf{A}_{\pi j}\}$, corresponding system of linear equations can be solved for $\boldsymbol{\pi}$ either uniquely or may have infinite number of solutions. In general, if the information matrix is rank-deficient, a general solution of the system (11) can be presented in the following form

$$\hat{\boldsymbol{\pi}} = \mathbf{A}_{\Sigma}^{+} \cdot \mathbf{B}_{\Sigma} + \left(\mathbf{I} - \mathbf{A}_{\Sigma}^{+} \mathbf{A}_{\Sigma} \right) \cdot \boldsymbol{\lambda} . \tag{21}$$

where the superscript "+" denotes the Moore–Penrose pseudoinverse, $\mathbf{A}_{\Sigma} = \sum_{j=1}^{m} \mathbf{A}_{\pi j}^{T} \boldsymbol{\eta}^{T} \boldsymbol{\eta} \mathbf{A}_{\pi j}$, $\mathbf{B}_{\Sigma} = \sum_{j=1}^{m} \mathbf{A}_{\pi j}^{T} \boldsymbol{\eta}^{T} \boldsymbol{\eta} \Delta \mathbf{t}_{\pi j}$ and $\boldsymbol{\lambda}$ is an arbitrary vector of the same size as $\boldsymbol{\pi}$. Using the later expression, all desired parameters contained in the vector $\boldsymbol{\pi}$ can be divided into the following groups [63]:

- **G1:** *Identifiable* parameters that can be obtained from (21) in unique way and are independent from the arbitrary vector $\boldsymbol{\lambda}$;
- **G2:** *Non-identifiable* parameters that cannot be computed uniquely from (21) and can take on any value without influence on the right-hand side of the equation (9), they correspond to the zero columns of the observation matrix $\mathbf{A}_{\pi}$;
- **G3:** *Semi-identifiable* parameters that are also cannot be computed uniquely but have influence on the right-hand side of the equation (9); they are united in subgroups where a single one can be treated as identifiable if the remaining ones are fixed.

To present typical examples of the parameters belonging to the groups G1, G2 and G3, it is possible to use the ideas similar to geometrical calibration. For instance, the elastostatic parameters of the actuated joints and adjacent links are redundant in their totality and belong to the group G3. Besides, if the loading direction cannot be altered, a number of parameters belong to the group G2 and cannot be identified from the corresponding experimental data. So, complete and irreducible model should contain all parameters from the group G1 and partially parameters of the group G3. More details on issue will be given in Section 4.3.

In this paper, in contrast to previous works, this classification is enhanced taking into account practical issues related to the limited precision of the measurement system. The main idea is to compare the absolute value of the estimated parameter with the range of possible fluctuations of the estimate caused by the measurement noise. For computational reasons, it is convenient to introduce a numerical indicator similar to the signal-to-noise ratio in communication, which is defined as follows

$$\nu_i = \left| \hat{\pi}_i \right| / \sigma_i , \quad i = 1, 2, ... \tag{22}$$

where σ_i is the standard deviation of the parameter estimate $\hat{\pi}_i$ extracted from the diagonal of the covariance matrix (16). It is clear that ν_i can be treated as the inverse of the relative accuracy, which allows us to avoid the problem of division by zero. In the following sections this indicator will be referred to as *parameter-to-noise ratio*.

Using the above defined indicator, the set of parameters belonging to the group G1 (theoretically identifiable) can be further divided into three subgroups:

- **G1+:** *Practically identifiable parameters*, for which the accuracy indicator is high: $\nu_i > \nu_0^{+}$; this subgroup describes principal elastostatic properties of the manipulator and should be certainly included in the reduced model used in the identification routines;
- **G1-:** *Practically non-identifiable parameters*, for which the accuracy indicator is low: $\nu_i < \nu_0^{-}$; this subgroup contains non-essential parameters that can be assigned to zero in the VJM-model without essential impact on its precision (in practice, the majority of these parameters are nominally equal to zero due to the physical nature of the compliance matrices);
- **G1~:** *Practically semi-identifiable parameters*, for which the accuracy indicator is intermediate: $\nu_0^{-} \le \nu_i \le \nu_0^{+}$; the parameters belonging to this subgroup are practically non-identifiable for the current experimental setup but, hypothetically, can be converted into practically identifiable ones by increasing the experiment number, improving the measurement precision of by modification of the measurement configurations.

An open question however is related to justified assigning of the upper and lower bounds ν_0^{+} and ν_0^{-}. From practical point of view that is adopted below, it is reasonable to use $\nu_0^{+} = 5$ and $\nu_0^{-} = 2$, which is in a good agreement with the quantiles of the normal distribution. However, the user may modify these values in accordance with the specificity of the problem of interest.

The above presented definitions allow us to revise the concept of "*suitable-for-calibration*" model that in previous works included all parameters of the group G1 (this model is also referred to as the "complete and irreducible" one). In this work, this model is limited to include only parameters of the subgroup G1+ (practically identifiable) that can be estimated with reasonable accuracy and provide good approximation of the original complete model. The following subsections address different aspects of model reduction allowing us to obtain the desired model suitable for the elastostatic calibration.

It should be noted that, in spite of the fact that the main focus of the paper is on the elastostatic modelling, similar ideas can be also successfully applied in manipulator geometric calibration.

4.2 Model reduction: physical approach ($\boldsymbol{\pi} \to \boldsymbol{\pi}'$)

Straightforward approach to the manipulator stiffness modelling leads to the exhaustive but redundant number of parameters to be identified. For instance, each links is described by a 6×6 matrix that includes 36 parameters that are treated as independent ones. However, as follows from physics, number of the pure physical and independent parameters is essentially lower (for a trivial prismatic beam, for example, there are only five physical parameters: three describing the geometry and two describing the material properties). Hence, there are strong relations between these 36 parameters but this fact is usually ignored in elastostatic calibration. Besides, due to fundamental properties of conservative system, the desired compliance matrices should be strictly symmetrical and positive-definite. In addition, for typical manipulator links, the compliance matrices are sparsed due to the shape symmetry with respect to some axis, but this property is also not taken into account in identification of the elastostatic parameters.

To take advantages of the compliance matrix properties and to increase the identification accuracy, two simple methods can be applied that allows us to reduce the number of parameters to be computed in the identification procedure (14). They can be treated as the physics-based model reduction techniques and formalised in the following way.

M1:**Symmetrisation.** For all compliance matrices $\mathbf{k}$ to be identified, replace the pairs of symmetrical parameters $\{k_{ij},\, k_{ji}\}$ by a single one $k_{ij},\, i<j$.

For each link, this reduction procedure is equivalent to re-definition of the model parameters vector in the following way

$$\boldsymbol{\pi} = \mathbf{M}\cdot\boldsymbol{\pi}' \tag{23}$$

where the binary matrix $\mathbf{M}$ of size 36×21 describes the mapping from the original to reduced parameter space. It can be proved that corresponding basic expression for the identification (9) can be rewritten as

$$\Delta\mathbf{t} = \mathbf{A}(\mathbf{q},\mathbf{w}\,|\,\boldsymbol{\pi}')\cdot\boldsymbol{\pi}' \tag{24}$$

where $\mathbf{A}(\mathbf{q},\mathbf{w}\,|\,\boldsymbol{\pi}') = \mathbf{A}(\mathbf{q},\mathbf{w}\,|\,\boldsymbol{\pi})\cdot\mathbf{M}$ denotes the reduced observation matrix. The later can be also computed as

$$\mathbf{A}(\mathbf{q},\mathbf{w}\,|\,\boldsymbol{\pi}') = [\mathbf{J}_\theta\boldsymbol{\omega}_1\mathbf{J}_\theta^T\mathbf{w},\ \mathbf{J}_\theta\boldsymbol{\omega}_2\mathbf{J}_\theta^T\mathbf{w},\ ...\mathbf{J}_\theta\boldsymbol{\omega}_{21}\mathbf{J}_\theta^T\mathbf{w}] \tag{25}$$

where $\boldsymbol{\omega}_1,\boldsymbol{\omega}_2,...$ denote the binary matrices of size 6×6 for which non-zero elements (i.e. equal to 1) are located in the following way: for the parameter π_l corresponding to the matrix elements $k_{ij},\, i\le j$, the non-zero elements are $\omega_{ij}=\omega_{ji}=1$. It is clear that this idea allows us to reduce the number of links compliance parameters from 36 to 21 (and from 258 to 153 for the entire 6 d.o.f. manipulator).

M2:**Sparcing.** For all compliance matrices $\mathbf{k}$ to be identified, eliminate from the set of unknowns the parameters k_{ij} corresponding to zeros in the stiffness matrix template $\mathbf{k}^0$ derived analytically for the manipulator link with similar shape.

To obtain a desired template matrix, is convenient to use any realistic link-shape approximation. For example using the trivial beam [69], the desired template can be presented as

$$\mathbf{k}^0 = \left[\begin{array}{ccc:ccc} * & 0 & 0 & 0 & 0 & 0 \\ 0 & * & 0 & 0 & 0 & * \\ 0 & 0 & * & 0 & * & 0 \\ \hdashline 0 & 0 & 0 & * & 0 & 0 \\ 0 & 0 & * & 0 & * & 0 \\ 0 & * & 0 & 0 & 0 & * \end{array}\right] \tag{26}$$

where the symbol "*" denotes non-zero elements. It allows further reducing the number of the unknown parameters from 21 to 8, taking into account only essential ones from physical point of view. It can be also proved that the template (26) is valid for any link whose geometrical shape is symmetrical with respect to three orthogonal axes. But it is necessary to be careful if this property is not kept strictly.

It should be stressed that the actuated joint compliances cannot be identified separately. So, they should be included in the compliance matrix of the previous link by means of modification of the corresponding diagonal elements.

M3:**Aggregation.** Eliminate from the set of model parameters the ones that corresponds to joint compliances before which there is an elastic link; in terms of parameters identifiability the compliance of those joints cannot be split from the links.

Summarizing these methods, it should be mentioned that the above presented approach essentially reduce the number of parameters to be identified (by the factor 4.5) but they do not violate such basic properties as the mode completeness, i.e. the ability to describe any deflection caused by the external loading. Below, these reduced set of the original model parameters $\boldsymbol{\pi}$

will be referred to as $\boldsymbol{\pi}'$. However, the obtained reduced model may still have some redundancy in the frame of entire manipulator, where the virtual springs of adjacent joints/actuators cause similar impact on the end-effector deflections under the loading.

To illustrate efficiency of the methods M1 and M2, the identification problem considered in section 3.2 have been solved for reduced set of the compliance parameters. It yielded the following result

$$\hat{\mathbf{k}} = \left[\begin{array}{ccc:ccc} -3.05\cdot10^{-8} & 0 & 0 & 0 & 0 & 0 \\ 0 & 8.05\cdot10^{-5} & 0 & 0 & 0 & 3.98\cdot10^{-4} \\ 0 & 0 & 3.64\cdot10^{-5} & 0 & -1.71\cdot10^{-4} & 0 \\ \hdashline 0 & 0 & 0 & 3.76\cdot10^{-3} & 0 & 0 \\ 0 & 0 & -1.71\cdot10^{-4} & 0 & 1.09\cdot10^{-3} & 0 \\ 0 & 3.98\cdot10^{-4} & 0 & 0 & 0 & 2.65\cdot10^{-3} \end{array}\right] \tag{27}$$

which is essentially better compared to (18). In particular, the identification errors for the most of the desired parameters are less than 0.4%, i.e. 4 times lower. The only exception is the small element $\hat{k}_{11}$ that is still negative and contradicts to the physical sense. This motivates further efforts to obtain reliable stiffness model whose parameters can be calibrated in real industrial environment.

From the geometrical calibration it is known that in spite of the fact that redundant model is suitable for direct and inverse computations it cannot be used in identification since the observation matrix does not have sufficient rank. Similar problem arises in elastostatic calibration where some stiffness matrix elements of adjacent links/joints are coupled and cannot be identified separately. The problem of construction complete and irreducible model has been widely studied in geometrical calibration and the developed techniques can be adopted for the elastostatic calibration.

4.3 Model reduction: algebraic approach ($\boldsymbol{\pi}' \to \boldsymbol{\pi}''$)

The physical approach described in the previous sub-section allows us essentially reducing the number of model parameters. However, it does not guarantee that the obtained model is suitable for calibrations (i.e. that the model is non-redundant and the number of parameters is equal to the observation matrix rank). In practice, the following inequality is often satisfied: $rank\left(\mathbf{A}_a\left(\mathbf{q}_a, \mathbf{w}_a \mid \boldsymbol{\pi}'\right)\right) < \dim\left(\boldsymbol{\pi}'\right)$. To overcome the problem, this sub-section presents some algebraic tools aimed at further reduction of the model parameter set from $\boldsymbol{\pi}'$ to $\boldsymbol{\pi}''$, which ensures full identifiability:

$$rank\left(\mathbf{A}_a\left(\mathbf{q}_A, \mathbf{w}_a \mid \boldsymbol{\pi}'\right)\right) = rank\left(\mathbf{A}_a\left(\mathbf{q}_a, \mathbf{w}_a \mid \boldsymbol{\pi}''\right)\right) = \dim\left(\boldsymbol{\pi}''\right) \tag{28}$$

These tools are based on the partitioning of the parameters set $\boldsymbol{\pi}'$ into three non-overlapping groups (identifiable, non-identifiable and semi-identifiable), which are either eliminated from the model or reduced to ensure the equality (28).

To introduce relevant algebraic technique, let us apply the SVD decomposition and present the aggregated observation matrix $\mathbf{A}_a\left(\mathbf{q}_a, \mathbf{w}_a \mid \boldsymbol{\pi}'\right)$ as the product of three matrices $\mathbf{U}\cdot\boldsymbol{\Sigma}\cdot\mathbf{V}^T$ (orthogonal, diagonal and orthogonal, respectively):

$$\left[\begin{array}{c} \mathbf{A}\left(\mathbf{q}_1, \mathbf{w}_1 \mid \boldsymbol{\pi}'\right) \\ \mathbf{A}\left(\mathbf{q}_2, \mathbf{w}_2 \mid \boldsymbol{\pi}'\right) \\ \cdots \\ \mathbf{A}\left(\mathbf{q}_{m_c}, \mathbf{w}_{m_c} \mid \boldsymbol{\pi}'\right) \end{array}\right] = \left[\mathbf{U}_1, \mathbf{U}_2, \ldots \mathbf{U}_m\right] \cdot \left[\begin{array}{ccc:c} \sigma_1 & 0 & 0 & \\ 0 & \sigma_2 & 0 & \mathbf{0}_{r\times n'} \\ & & & \\ 0 & 0 & \sigma_r & \\ \hdashline & \mathbf{0}_{m'\times r} & & \mathbf{0}_{m'\times n'} \end{array}\right] \cdot \left[\begin{array}{c} \mathbf{V}_1^T \\ \mathbf{V}_2^T \\ \\ \mathbf{V}_n^T \end{array}\right] \tag{29}$$

Here $\mathbf{U} = [\mathbf{U}_1, \mathbf{U}_2, \ldots \mathbf{U}_m]$ and $\mathbf{V} = [\mathbf{V}_1, \mathbf{V}_2, \ldots \mathbf{V}_v]$ are orthogonal matrices of the size $m \times m$ and $n \times n$ respectively whose columns are denoted as $\mathbf{U}_i$ and $\mathbf{V}_j$; the second factor $\boldsymbol{\Sigma}$ is a rectangular diagonal matrix of the size $m \times n$ containing r positive real numbers $\sigma_1, \sigma_2, \ldots \sigma_r$ in descending order; $m = \dim\left(\Delta\mathbf{t}_a\right)$ is the number of rows in the observation matrix (i.e. number of equations used for the identification), $n = \dim\left(\boldsymbol{\pi}'\right)$ is current number of the model parameters, and r is the rank of the aggregated observation matrix, $m' = m - r$, $n' = n - r$. It is clear that r defines the maximum number of parameters that can be identified using given set of manipulator configurations $\{\mathbf{q}_i\}$ and corresponding wrenches $\{\mathbf{w}_i\}$.

Further, after substitution (29) into (12) and left-multiplication by $\mathbf{U}^T$, the original system of m identification equations (12) can be rewritten as

$$\left[\begin{array}{cccc:c} \sigma_1 & 0 & \ldots & 0 & \\ 0 & \sigma_2 & \ldots & 0 & \mathbf{0}_{r\times n'} \\ \ldots & \ldots & \ddots & \ldots & \\ 0 & 0 & \ldots & \sigma_r & \\ \hdashline \multicolumn{4}{c:}{\mathbf{0}_{m'\times r}} & \mathbf{0}_{m'\times n'} \end{array}\right] \cdot \begin{bmatrix} \mathbf{V}_1^T \\ \mathbf{V}_2^T \\ \ldots \\ \mathbf{V}_n^T \end{bmatrix} \cdot \boldsymbol{\pi}' = \begin{bmatrix} \mathbf{U}_1^T \\ \mathbf{U}_2^T \\ \ldots \\ \mathbf{U}_m^T \end{bmatrix} \cdot \Delta\mathbf{t}_a \tag{30}$$

where the number of equation is equal to n and perfectly corresponds to the vector $\boldsymbol{\pi}'$ dimension (it is obvious that $n \le m$). Taking into account particularities of the sparse matrix $\boldsymbol{\Sigma}$ (with r non-zero elements only), it is possible to rewrite the system (30) in the form

$$\begin{aligned} &\sigma_i \cdot \mathbf{V}_i^T \cdot \boldsymbol{\pi}' = \mathbf{U}_i^T \cdot \Delta\mathbf{t}_a; \qquad i = 1,2,...,r \\ &0 \cdot \mathbf{V}_i^T \cdot \boldsymbol{\pi}' = \mathbf{U}_i^T \cdot \Delta\mathbf{t}_a; \qquad i = r+1,...,n \end{aligned} \tag{31}$$

where the second group of $m' = m - r$ equations should be excluded from further consideration because relevant residuals do not depend on the parameters of interest $\boldsymbol{\pi}'$ (since they are multiplied by zero matrix). It can be proved that $\mathbf{U}_i^T \cdot \Delta\mathbf{t}_a \equiv \mathbf{0}$ for $i > r$ if the measurement vector $\Delta\mathbf{t}_a$ does not contain noise. It is also worth mentioning that for real identification problems (with the measurement noise), the second group of equations produces constant residuals that cannot be minimised in the least-square objective (13) by varying the vector of unknown parameters $\boldsymbol{\pi}'$.

Hence, for the identification of n parameters included in the vector $\boldsymbol{\pi}'$, a system of r linear equations have been obtained that cannot be solved uniquely in a general case. Its partial solution can be found by dividing on $\sigma_i > 0$ each of r linear equations $\sigma_i \cdot \mathbf{V}_i^T \cdot \boldsymbol{\pi}' = \mathbf{U}_i^T \cdot \Delta\mathbf{t}_a$ and further straightforward multiplication of the left and right sides by the matrix $\left[\mathbf{V}_1, \mathbf{V}_2, ..., \mathbf{V}_r\right]$, which yields

$$\left[\mathbf{V}_1, \mathbf{V}_2, ..., \mathbf{V}_r\right] \begin{bmatrix} \mathbf{V}_1^T \\ \mathbf{V}_2^T \\ \ldots \\ \mathbf{V}_r^T \end{bmatrix} \cdot \boldsymbol{\pi}' = \left[\mathbf{V}_1, \mathbf{V}_2, ..., \mathbf{V}_r\right] \begin{bmatrix} \mathbf{U}_1^T / \sigma_1 \\ \mathbf{U}_2^T / \sigma_2 \\ \ldots \\ \mathbf{U}_r^T / \sigma_r \end{bmatrix} \cdot \Delta\mathbf{t}_a \tag{32}$$

Using the first set of r equations of system (31) one can obtain partial solution of system (30)

$$\boldsymbol{\pi}'_0 = \sum_{i=1}^{r} \left(\sigma_i^{-1}\ \mathbf{V}_i \cdot \mathbf{U}_i^T\right) \cdot \Delta\mathbf{t}_a \tag{33}$$

This allows us to present the general solution (21) as the sum of this partial solution and an arbitrary vector from the subspace with the basis $\mathbf{V}_{r+1}, \mathbf{V}_{r+2}, ...\mathbf{V}_n$

$$\hat{\boldsymbol{\pi}}' = \boldsymbol{\pi}'_o + \sum_{i=r+1}^{n} \lambda_i \mathbf{V}_i \tag{34}$$

where λ_i, $i = \overline{r+1, n}$ are arbitrary real values.

Hence, as follows from analysis of (31) and (34), depending on the properties of the matrix $\mathbf{V}$, all model parameters $\boldsymbol{\pi}'$ can be partitioned into three groups: G1 – *identifiable* parameters that are uniquely defined by the equation (34) and do not depend on the arbitrary values λ_i, for these parameters the corresponding row of the sub-matrix $[\mathbf{V}_{r+1}, ..., \mathbf{V}_m]$ is equal to zero; G2 – *non-identifiable* parameters that do not effect the residuals of system (31), for these parameters the corresponding row of the sub-matrix $[\mathbf{V}_1, ..., \mathbf{V}_r]$ is equal to zero; G3 – *semi-identifiable* parameters that effect the residuals but cannot be identified uniquely, couplings between these parameters is defined by the vectors $\mathbf{V}_i$, $i = \overline{1, r}$. Thus, based on this decomposition, the algebraic-based model reduction techniques can be formalised in the following way:

M4a:**Partitioning.** Divide the reduced set of the model parameters $\boldsymbol{\pi}'$ into three non-overlapping groups G1, G2 and G3 in accordance with the following rules applied to all π'_i, $i = \overline{1, \dim(\boldsymbol{\pi}')}$:

Rule 1: Include the parameter π'_i into the group G1 if the *i*th row of the sub-matrix $[\mathbf{V}_{r+1}, ..., \mathbf{V}_m]$ is equal to zero;

Rule 2: Include the parameter π'_i into the group G2 if the *i*th row of the sub-matrix $[\mathbf{V}_1, ..., \mathbf{V}_r]$ is equal to zero;

Rule 3: If the parameter π'_i is not included in G1 or G2, include it in the group G3.

M4b:**Elimination.** Eliminate from the set of unknowns (model parameters) non-identifiable parameters that correspond to group G2.

After application of these methods, the current set of model parameters $\boldsymbol{\pi}'$ is reduced to the sub-set $\{\boldsymbol{\pi}' \setminus \boldsymbol{\pi}_{G2}\}$ that does not influence the rank of the observation matrix, i.e. $rank\left(\mathbf{A}_a\left(\mathbf{q}_a, \mathbf{w}_a \mid \{\boldsymbol{\pi}' \setminus \boldsymbol{\pi}_{G2}\}\right)\right) = rank\left(\mathbf{A}_a\left(\mathbf{q}_a, \mathbf{w}_a \mid \boldsymbol{\pi}'\right)\right)$. Nevertheless, relevant model may be redundant yet, i.e. $rank\left(\mathbf{A}_a\left(\mathbf{q}_a, \mathbf{w}_a \mid \{\boldsymbol{\pi}' \setminus \boldsymbol{\pi}_{G2}\}\right)\right) < \dim\left(\{\boldsymbol{\pi}' \setminus \boldsymbol{\pi}_{G2}\}\right)$. It should be noted that $rank\left(\mathbf{A}_a\left(\mathbf{q}_a, \mathbf{w}_a \mid \boldsymbol{\pi}_{G1}\right)\right) = \dim\left(\boldsymbol{\pi}_{G1}\right)$ while $rank\left(\mathbf{A}_a\left(\mathbf{q}_a, \mathbf{w}_a \mid \boldsymbol{\pi}_{G3}\right)\right) < \dim\left(\boldsymbol{\pi}_{G3}\right)$. So, another, and the most difficult problem that arises after M4, is to define the sub-set of identifiable parameters inside of $\boldsymbol{\pi}_{G3}$ (the remaining ones should be set to constant values).

It is clear that the above mentioned problem has infinite number of solutions. Let us presents an algorithm that is able to split the set of parameters $\boldsymbol{\pi}_{G3}$ into the non-overlapping groups of coupled parameters $\boldsymbol{\pi}_{G3}^j$ and than choose identifiable one from the group based on their physical scene:

M5a:Splitting. Split the set of semi-identifiable model parameters $\boldsymbol{\pi}_{G3}$ into the non-overlapping groups of coupled parameters $\boldsymbol{\pi}_{G3}^j$ for which the following conditions are satisfied:

(a) $\boldsymbol{\pi}_{G3} = \boldsymbol{\pi}_{G3}^1 \bigcup \boldsymbol{\pi}_{G3}^2 \bigcup .... \boldsymbol{\pi}_{G3}^m$, $\boldsymbol{\pi}_{G3}^i \bigcap \boldsymbol{\pi}_{G3}^j = \varnothing \;\; \forall \; i \neq j$;

(b) $rank\left(\mathbf{A}_a\left(\mathbf{q}_a, \mathbf{w}_a \mid \boldsymbol{\pi}_{G3}^i\right)\right) = rank\left(\mathbf{A}_a\left(\mathbf{q}_a, \mathbf{w}_a \mid \boldsymbol{\pi}_{G3}^i \setminus \boldsymbol{\pi}_{G3}^i(j)\right)\right) \;\; \forall \; j = \overline{1 : \dim(\boldsymbol{\pi}_{G3}^i)}$

(c) $rank\left(\mathbf{A}_a\left(\mathbf{q}_a, \mathbf{w}_a \mid \boldsymbol{\pi}_{G3}^i\right)\right) < rank\left(\mathbf{A}_a\left(\mathbf{q}_a, \mathbf{w}_a \mid \boldsymbol{\pi}_{G3}^i \quad \boldsymbol{\pi}_{G3}^j(k)\right)\right) \;\; \forall \; i \neq j, k = \overline{1 : \dim(\boldsymbol{\pi}_{G3}^j)}$

In practice, when this grouping is not evident, it is possible to use numerical technique, which is based on the SVD-decomposition of the reduced observation matrix $\mathbf{A}_a\left(\mathbf{q}_a, \mathbf{w}_a \mid \boldsymbol{\pi}_{G3}\right)$. Using similar notation, the matrix $\mathbf{V}$ can be presented as $\mathbf{V} = \left[\mathbf{V}_1, \mathbf{V}_2, ...\right]$ in accordance with the rank of $\mathbf{A}_a\left(\mathbf{q}_a, \mathbf{w}_a \mid \boldsymbol{\pi}_{G3}\right)$. So, the couplings between the elements are defined by the sub-matrix $\left[\mathbf{V}_1, \mathbf{V}_2, ..., \mathbf{V}_r\right]$. One of the easiest ways to find the desired couplings is to compute the matrix

$$\mathbf{L} = \left(\left[\mathbf{V}_1, \mathbf{V}_2, ..., \mathbf{V}_r\right]^*\right)^{-1} \cdot \begin{bmatrix} \mathbf{V}_1^T \\ \mathbf{V}_2^T \\ ... \\ \mathbf{V}_r^T \end{bmatrix} \tag{35}$$

where the symbol "*" denotes operation of the row selection that conserve the matrix rank. The latter leads to a full-rank square matrix presented above as the firs term of (35). It should be noted that this operation is not unique, nevertheless, it allows to obtain the couplings between the model parameters described by the sparse matrix $\mathbf{L}$. Then, the desired groups of parameters can be easily detected after transformation $\mathbf{L}$ into the block-diagonal form.

Using the above presented idea, the next step can be presented as follows:

M5b:Selection. In each group of parameters $\boldsymbol{\pi}_{G3}^j$, specify $n_j = rank\left(\mathbf{A}_a\left(\mathbf{q}_a, \mathbf{w}_a \mid \boldsymbol{\pi}_{G3}^i\right)\right)$ parameters that will be treated as identifiable

M5c:**Assigning.** In each group of parameters $\boldsymbol{\pi}_{G3}^j$, fix remaining $m_j = \dim\left(\boldsymbol{\pi}_{G3}^j\right) - rank\left(\mathbf{A}_a\left(\mathbf{q}_a, \mathbf{w}_a \mid \boldsymbol{\pi}_{G3}^i\right)\right)$ parameters to some constants; these parameters will be treated as non-identifiable

It should be noted that the sequence of methods M5b and M5c is not strict; identifiable and non-identifiable parameters can be selected and fixed iteratively, using the methods M5b and M5c several times. After application of the methods M5a, M5b and M5c, the set of parameters $\boldsymbol{\pi}_{G3}$ is split into two subsets: the subset of the parameters that will be treated as identifiable $\boldsymbol{\pi}_{G3}^{id}$ and subset that will be treated as non identifiable ones $\boldsymbol{\pi}_{G3}^{ni}$ and will be assigned to some constant values ($\boldsymbol{\pi}_{G3}^{ni} = const$); i.e. $\boldsymbol{\pi}_{G3}^{id} \bigcup \boldsymbol{\pi}_{G3}^{ni} = \boldsymbol{\pi}_{G3}$, $\boldsymbol{\pi}_{G3}^{id} \bigcap \boldsymbol{\pi}_{G3}^{ni} = \varnothing$.

As the result of algebraic approach, the complete set of parameters $\boldsymbol{\pi}'$ is reduced to $\boldsymbol{\pi}''$, It includes all parameters from the group G1 and assigned-to-be-identifiable ones from the group G3. It is clear that the presented algebraic methods do not violate the model completeness, i.e. $rank\left(\mathbf{A}_a\left(\mathbf{q}_a, \mathbf{w}_a \mid \boldsymbol{\pi}''\right)\right) = rank\left(\mathbf{A}_a\left(\mathbf{q}_a, \mathbf{w}_a \mid \boldsymbol{\pi}'\right)\right)$.

4.4 Model reduction: statistical approach ($\boldsymbol{\pi}'' \rightarrow \boldsymbol{\pi}'''$)

As follows from relevant study and above presented example, rigorous reduction methods based on the physical and mathematical properties of the compliance matrix are rather limited if the measurement noise is non- negligible. This gives us reasons to develop some heuristic rules that take into account the measurement noise impact on the identification accuracy. It is clear that extremely low accuracy is not acceptable, but often corresponding parameters are so small that their influence on the end-effector deflections is very small. This supports an idea for heuristic reduction of small model parameters but leaving an open problem of their further reconstruction in the VJM-model using some empirical or semi-empirical relations induced by mathematical relations between the stiffness matrix elements.

To take into account the relative accuracy of the parameter estimates, it is convenient to use a simple indicator showing parameter-to-noise ratio (22) introduced in sib-section 4.1. It is evident that it should be applied only to those parameters that

belong to the group G1 (theoretically identifiable). Using this index, a heuristic model reduction technique allowing us to distinguish the practically identifiable parameters from the hardly-identifiable ones can be formalised as follows:

M6:**Neglecting.**

Step 1: Using complete but non-redundant model derived after application of physical and algebraic model reduction techniques, compute estimates of the desired parameters $\hat{\boldsymbol{\pi}}'$ and their covariance matrix $\mathrm{cov}(\hat{\boldsymbol{\pi}}')$ by means of equations (14) and (16);

Step 2: Using the parameters estimates $\hat{\boldsymbol{\pi}}'$ and the diagonal elements of the covariance matrix $\mathrm{cov}(\hat{\boldsymbol{\pi}}')$, compute the parameter-to-noise ratios ν_i in accordance with expression (22);

Step 3. For all compliance matrices $\mathbf{k}$ to be identified, eliminate from the set of unknowns the parameters k_{ij} for which parameter-to-noise ratios ν_{ij} is lower the user defined threshold: $\nu_{ij} < \nu_0^+$.

This method allows us to eliminate from the model the parameters whose identification accuracy is comparable with the noise impact and, strictly speaking, these values cannot be considered as reliable estimates of k_{ij}.

As follows from our experience, it a very powerful method with two useful features: (i) elimination of small (but theoretically non-zero) parameters, and (ii) detection of elements corresponding to zeros in the matrix template (see method M2), if the latter has been defined rather carefully. These conclusions are clearly confirmed by the numerical example presented in section 3.2 (see (19) and (20)). In this example, it is worth to pay attention to the element $\hat{k}_{11}$ that is really small for the majority of manipulator links (because the link length is always essentially higher compared to the cross-section dimensions). Elimination of this parameter is really negligible for the manipulator Cartesian stiffness matrix (7) that integrates impact of all compliance elements. Nevertheless, after identification, the parameter $\hat{k}_{11}$ can be reconstructed approximately using non-zero elements of the compliance matrix and some relations between $\hat{k}_{ij}$ induced by physics. The last problem is currently under study but is not in the scope of this paper.

In conclusion of this section, it should be noted that the proposed methods M1-M5 allow us essentially reducing the number of model parameters while retaining the model accuracy. For example, for 6 d.o.f. manipulator, the number of parameters is reduced from 258 to 42 allowing us to obtain an adequate stiffness model in real industrial environment.

5 Illustrative example

To illustrate utilisation and the efficiency of the developed model reduction technique this section proposes detailed example that describes step-by-step application of the proposed model reduction methods. It deals with the identification of elasto-static parameters of a 6 dof manipulator.

5.1 Basic assumptions and model description

Let us consider a typical 6 dof serial manipulator with 6 rotational actuated joints whose geometric model is presented in Figure 3. It is assumed that all manipulator components (both actuated joints and links) are subject to the elastic deformations under the influence of the external force/torque. For this manipulator, a complete elastostatic model contains 258 parameters that describe compliance of 7 links (defined by 6×6 stiffness matrices) and 6 actuated joints (defined by stiffness coefficients).

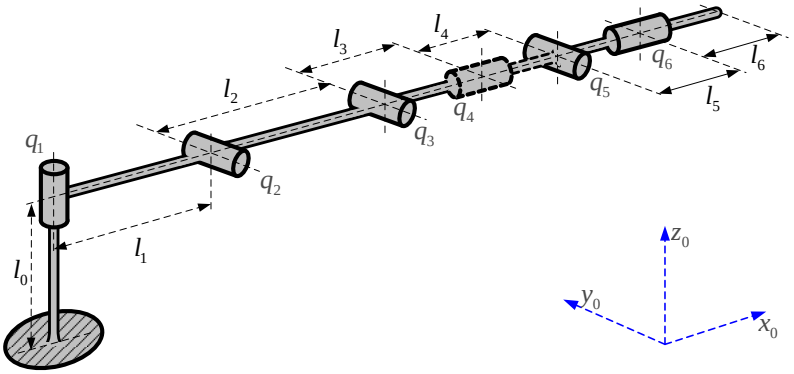

Figure 3 Kinematic model of the considered 6 dof manipulator

It is assumed that each manipulator link has regular hollow circular cross-section and its stiffness matrix can be computed using classical expression [69]. All physical parameters that are required to compute the complete elastostatic model are given in Table 1. It is also assumed that all actuated joints have the same compliance coefficients that are equal to $10^{-6}\,rad\,/\,N\cdot m$. These

data allows us to construct a quasi-diagonal stiffness matrix $\mathbf{K}_\theta$ of size 48×48 that incorporates all 7 above mentioned matrices of size 6×6 and 6 scalar coefficients.

Table 1 Principal parameters of the considered 6 dof manipulator

Parameters	Link #0	Link #1	Link #2	Link #3	Link #4	Link #5	Link #6
Link length, m	0.7	0.4	1.2	0.8	0.3	0.2	0.2
External diameter, m	0.12	0.12	0.12	0.12	0.12	0.12	0.12
Internal diameter, m	0.10	0.10	0.10	0.10	0.10	0.10	0.10
Material properties	Young's modulus $E = 7\cdot10^{10}$ N / m^2, Poisson's ratio $\nu = 0.346$						

To take into account limited precision of the measurement system, it is assumed that both and position and orientation of the end-effector are available for the identification, with accuracy $25\mu m$ and $250\mu rad$ respectively (this corresponds to a typical industrial laser-tracker measurement system). It is evident that here each calibration experiment requires two measurements (with and without external loading), which increase the measurement noise impact by the factor $\sqrt{2}$.

In order to identify all 258 desired parameters it is required at least $\lceil 258/36 \rceil = 8$ measurement configurations, each of which is used for six calibration experiments with different external wrenches. To simplify relevant expressions, the exciting forces/torques were directed along the Cartesian axes and their magnitudes were set to 1000 N and 1000 $N\cdot m$, respectively. For this example, the measurement configurations were generated randomly and their number was increased up to 18 to ensure sufficient rank of the observation matrix. So, here calibration is based on 108 virtual experiments each of which provides 6 end-effector deflections. In total, it gives 648 scalar equations that will be used for identification of the model parameters (their number will be gradually reduced from 258 to 27).

5.2 Model reduction

As was mentioned above, a complete stiffness model of the considered 6 dof manipulator contains 258 different parameters that describe the compliance of 6 actuated joints and 7 manipulator links. After application of **M1** (physical approach, symmetrisation), the number of the model parameters is reduced down to 153 (that corresponds to 21 parameters for each 6×6 stiffness matrix describing the link elasticity). At the next step, after applying of **M2** (physical approach, sparcing) the number of parameters is reduced to 64, which corresponds to 8 parameters per a stiffness matrix of size 6×6. Finally, using **M3** (aggregation) that integrates the joint compliance coefficients in the link stiffness matrices, the number of desired parameters becomes equal to 56. Hence, the physical model reduction methods M1-M3 allowed us to reduce the number of the model parameters by the factor 4.6.

Table 2 Identifiable parameters of manipulator elastostatic model ("*" denotes strictly identifiable parameter, "+" corresponds to a semi-identifiable parameter included in the reduced model).

	k_{11}	k_{22}	k_{33}	k_{44}	k_{55}	k_{66}	k_{26}	k_{35}
Link #0	+	+	+	+	+	+	*	*
Link #1	+			+	+	+		
Link #2	+			+	+	+		
Link #3	+			+	+		*	
Link #4		+			+	+	+	
Link #5	+			+	+		*	
Link #6		+			+	+	+	

Further, for the obtained set of the model parameters, the rank of corresponding 648×56 observation matrix was evaluated. It was equal to 32, which means that 24 parameters among 56 cannot be identified. The latter motivates application of the algebraic model reduction methods. After application of **M4** (partitioning and elimination), the current set of the model parameters was split into 3 principal groups, where only 4 parameters are strictly identifiable and remaining 52 are semi-identifiable (there are no strictly non-identifiable parameters on this stage). Using these data, the method **M5** allowed us to reduce the parameters number down to 32. Corresponding selection process was based on giving priority to the joint compliances and diagonal elements of the stiffness matrices. Relevant results are presented in Table 2.

To reduce the measurement noise impact on the model validity, the obtained complete non-redundant model (with 32 parameters) was further reduced. On this step, a number of relatively small model parameters were detected using method **M6** (statistical approach). For this purpose, the parameter-to-noise ratios were computed and compared with the threshold level. Relevant results are presented in Table 3. As follows from this table, varying the threshold level from 1 to 5, the number of the model parameters can be reduced down to from 27 to 25. In the following sub-section it will be shown that threshold level equal to 2 (corresponding to the model with 27 parameters) ensures acceptable model accuracy. Summary of the presented model reduction process is given in Table 4.

Table 3 Parameter-to-noise ratios for complete non-reducible model (relatively small parameters are highlighted).

	k_{11}	k_{22}	k_{33}	k_{44}	k_{55}	k_{66}	k_{26}	k_{35}
Link #0	173	160	141	246	163	218	174	193
Link #1	14			36	103	0.2		
Link #2	510			548	176	253		
Link #3	39			235	48		110	
Link #4		0.7			10	15	0.3	
Link #5	2.5			35	3.2		6.6	
Link #6		0.3			7.1	5.1	0.4	

Table 4 Summary of the elasto-static model reduction process for 6 dof serial manipulator

Approach	Step	Model description	Number of parameters
Original model		6 joints +7 links (36 parameters per link)	258
Physical	M1: Symmetrisation	6 joints +7 links (21 parameters per link)	153
	M2: Sparcing	6 joints +7 links (8 parameters per link)	62
	M3: Aggregation	7 links (8 parameters per link)	56
Algebraic	M4a:Partitioning M4b:Elimination	G1: Identifiable parameters – 4 G2: Non-identifiable parameters - 0 G3: Semi-identifiable parameters – 52	52
	M5a:Splitting M5b:Selection M5c:Assigning	Selection of 28 independent parameters from 52 semi-identifiable ones	32
Statistical	M6: Neglecting	Threshold level equal to 2	27

5.3 Comparison analysis

To demonstrate validity of the developed technique, the obtained model has been used for the prediction of the manipulator compliance errors and their compensation. It is worth mentioning that for the considered experimental setup, the end-effector deflections due to external forces/torques are non-negligible and vary from 2 to 35 mm. For comparison purposes, the compliance error compensation accuracy was evaluated for two elasto-static models: (i) *complete irreducible model* with 32 parameters, and (ii*) reduced model* with 27 parameters that corresponds to the threshold level equal to 2. Relevant analysis was based on the randomly generated set of configurations, which is different from one used on the identification step. Corresponding simulation results are presented in Table 5.

Table 5 Compliance error compensation efficiency for full and reduced set of model parameters

		Residuals			
		Coordinate-based		Distance-based	
		max	RMS	max	RMS
Deflections magnitude, [mm]		33.9	9.3	34.8	16.7
Deflections prediction errors, [μm]	Complete model (32 parameters)	8.4	2.8	11.1	4.6
	Reduced model (27 parameters)	8.0	2.6	10.7	4.6

As follows from Table 5, neglecting of small elastic parameters is reasonable here and does not influence the efficiency of the compliance errors compensation. Moreover, for the considered configurations, the reduced model allowed us even to improve slightly the positioning accuracy (by 5%). It is clear that this result cannot be treated as a strict proof, but it was confirmed by numerous simulations for other configuration sets. Hence, the obtained reduced model is simple and robust with respect to the measurement noise while ensuring almost the same accuracy as the complete stiffness model for the manipulator compliance error compensation.

6 Application example: calibration of industrial robot Kuka KR-270

To demonstrate benefits of the developed techniques for industrial applications, this section deals with the elastostatic and geometric calibration of industrial robot Kuka KR-270 (Figure 5) employed in high precession machining of aircraft parts. It contains relevant experimental results and their comparatives analysis.

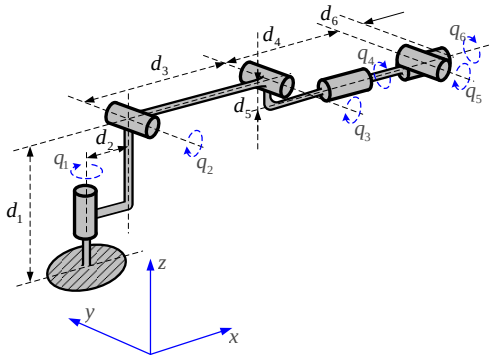

(a) Industrial robot KUKA KR270 (b) The manipulator architecture

Figure 4 Industrial robot KUKA KR270 and its cinematic model.

6.1 Elastostatic calibration

For the considered application area, the technological process generates essential interaction between the workpiece and manipulator, which causes non-negligible deflections of the end-effector. To compensate related positioning errors on the control level (via adjusting a target trajectory [4]), an accurate but simple enough elasto-static model is required. In practice, the desired model is not usually provided by robot manufactures and should be obtained from dedicated experimental study. Let us apply the developed technique to get the desired model and to identify its parameters in real industrial environment.

The considered manipulator contains 7 links separated by 6 actuated joints. Taking into account that in general the elastostatic properties of each link are defined by 6x6 stiffness matrix, the complete but obviously redundant model contains 258 parameters. As a result of application model reduction techniques (M1-M5), the number of parameters to be identified has been reduced down to 26. More details on each step are given in Table 6. Additional restrictions here are caused by the partial-pose measurement technique and the gravity-based loading generating the desired deflections. Relevant experimental setup is presented in Figure 5. Because of such measurement method, 10 elastostatic parameters are not identifiable from the available measurement data (Table 7). The manipulator configurations for the elastostatic calibration were generated using the design of experiments and previously developed test-pose technique, which is based on the industry-oriented performance measure [57]. It should be noted that for the considered experimental setup and selected measurement configurations, all model parameters in complete and irreducible model are practically identifiable. This fact confirms the importance of the measurement configurations selection that directly affects

model parameters identifiably in real industrial environment. Another particularity of the industrial robot KUKA KR270 that should be taken into account in an accurate elasto-staic model is a gravity compensator that is attached in parallel to the second actuated joint. Its equivalent model was presented in [35]. In the frame of the complete and irreducible model, the gravity compensator impact is taken into account by introducing a configuration dependant virtual spring in the second joint. More details on this approach are given in [35].

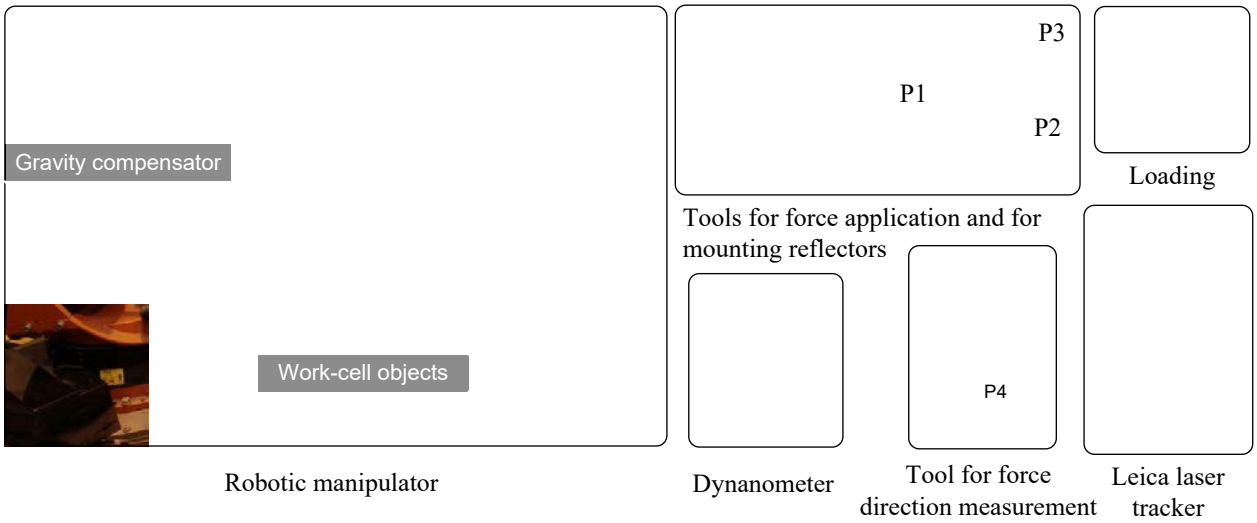

Figure 5 Experimental setup for elastostatic calibration

Table 6 Summary of the elasto-static model reduction process for industrial robot Kuka KR-270 (without gravity compensator)

Approach	Step	Model description	Number of parameters
Original model		6 joints +7 links (36 parameters per link)	258
Physical	M1: Symmetrisation	6 joints +7 links (21 parameters per link)	153
	M2: Sparcing	6 joints +7 links (8 parameters per link)	62
	M3: Aggregation	7 links (8 parameters per link)	56
Algebraic	M4a:Partitioning M4b:Elimination	G1: Identifiable parameters – 1 G2: Non-identifiable parameters - 10 G3: Semi-identifiable parameters – 45	46
	M5a:Splitting M5b:Selection M5c:Assigning	Selection of 25 independent parameters from 45 semi-identifiable ones	26
Statistical	M6: Neglecting	Threshold level equal to 2	26

For the comparison purposes, calibration was performed using several elastostatic models that differ in their basic assumptions: (i) complete irreducible stiffness model, (ii) stiffness model with practically identifiable parameters and (iii) conventional model for the manipulator with rigid links and compliant actuated joints. All models have been examined with and without taking into account the effect of the gravity compensator. The obtained results are summarised in Table 8 showing capability to compensate the compliance errors using different elastostatic models. Graphical comparison of these results is given in Figure 6. As follows from them, the lowest compliance errors can be achieved using the model R2 (obtained using the developed model reduction technique), which ensures the positional accuracy 0.21 mm. In contrast, the conventional elasto-static model with rigid links gives accuracy 3.5 times worse comparing to model R2. The histograms of the errors distribution for the model R2 (Figure 7) show that the non-compensated compliance errors in all directions are unbiased and almost normally distributed.

Table 7 Parameter-to-noise ratios for complete non-reducible elasto-static model for industrial robot Kuka KR-270.

	k_{11}	k_{22}	k_{33}	k_{44}	k_{55}	k_{66}	k_{26}	k_{35}
Link #0	-	-	8.4	228	195	-	-	10.4*
Link #1	-	-		261	239	-	-	
Link #2		-	105	52.5	84.0	54.4		
Link #3		-	134	18.1	17.6	18.8	34.6	140
Link #4					35.6		10.5	
Link #5		10.6	43.9	19.4			21.1	35.1
Link #6		19.3			18.5		18.8	

Superscript "*" marks identifiable parameter, Symbols "-" indicate non-identifiable parameters by

Table 8 Efficiency of the compliance errors compensation using complete and reduced models.

Stiffness model	**Number of parameters**	**Compliance errors, mm**							
		x-direction		**y-direction**		**z-direction**		**positional**	
		MAX	RMS	MAX	RMS	MAX	RMS	MAX	RMS
Deflections magnitude without compensation		2.51	1.03	3.14	1.02	8.14	1.91	8.18	4.58
Complete model C1	26	0.27	0.10	0.43	0.13	0.38	0.12	0.45	0.22
Complete model C2	30	0.28	0.10	0.45	0.14	0.32	0.11	0.49	0.21
Reduced model R1	26	0.27	0.10	0.43	0.13	0.38	0.12	0.45	0.22
Reduced model R2	30	0.28	0.10	0.45	0.14	0.32	0.11	0.49	0.21
Conventional model J1	5	1.42	0.43	1.73	0.41	0.66	0.23	1.78	0.75
Conventional model J2	9	1.42	0.42	1.73	0.42	0.49	0.19	1.76	0.73

Model C1: Complete irreducible stiffness model without gravity compensator

Model C2: Complete irreducible stiffness model with gravity compensator

Model R1: Stiffness model with practically identifiable parameters ($\nu_i \geq 2$), without gravity compensator

Model R2: Stiffness model with practically identifiable parameters ($\nu_i \geq 2$), with gravity compensator

Model J1: Conventional model for the manipulator with rigid links and compliant actuated joints, without gravity compensator

Model J2: Conventional model for the manipulator with rigid links and compliant actuated joints, with gravity compensator

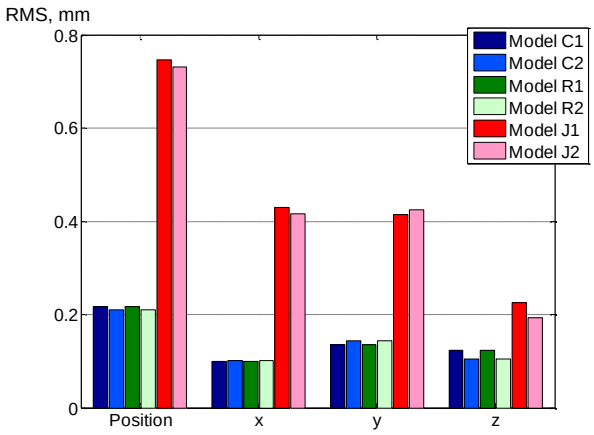

Figure 6 Efficiency of the compliance errors compensation using complete and reduced models

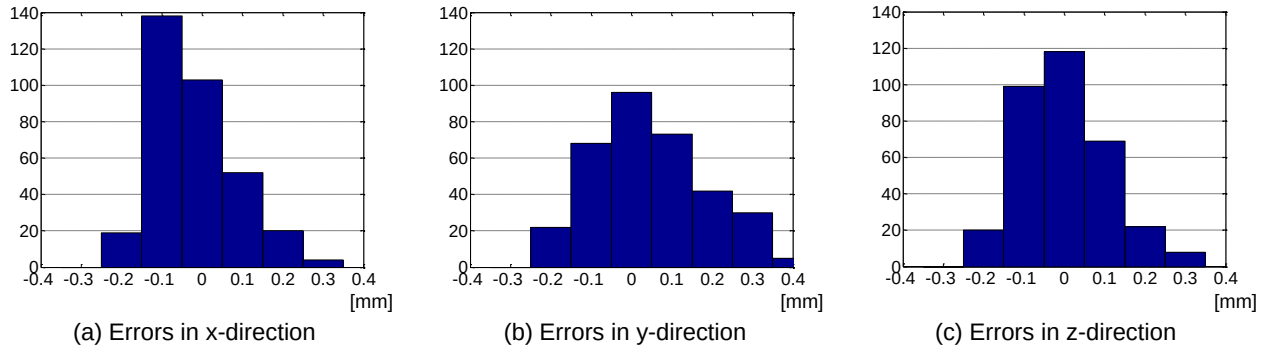

Figure 7 Statistical distribution of compliance errors after compensation (Model R2)

Hence, using the developed low-order stiffness model for the compliance error compensation gives essential improvement of the precision for the robotic based milling. It allowed us to compensate more than 95% of deflections caused by external loading and to guarantee the precision of about 0.2 mm under the loading of 2.5 kN (it is comparable with the robot repeatability of 0.06 mm).

6.2 Geometric calibration

In spite that main theoretical results have been developed for elastostatic calibration, they can be also used for the geometric case. Let us apply them to the geometric calibration of the industrial robot KUKA KR-270 (Figure 4) considered in the previous sub0section. As follows from the literature [8], a complete (and irreducible) geometric model for this robot contains 30 parameters ($4n_R + 2n_P + 6$, where n_R and n_P is the number of revolute and prismatic joints, respectively). Among them, 6 parameters describe the base transformation and 6 parameters define the tool transformation. They can be excluded from this study since usually a dedicated techniques is applied to identify them separately. So, theoretically identifiable geometric model for the considered manipulator includes 18 principle parameters that are collected in a single vector

$$\boldsymbol{\pi} = \left\{ p_{x1}\ p_{y1}\ \varphi_{x1}\ \Delta q_2\ p_{x2}\ \varphi_{x2}\ \varphi_{z2}\ \Delta q_3\ p_{x3}\ p_{z3}\ \varphi_{z3}\ \Delta q_4\ p_{y4}\ p_{z4}\ \varphi_{z4}\ \Delta q_5\ p_{z5}\ \varphi_{z5} \right\} \tag{36}$$

where Δq_j is the joint offset, p_{xj}, p_{yj}, p_{zj} and $\varphi_{xj}, \varphi_{yj}, \varphi_{zj}$ are the relevant translational and rotational parameters, and j indicates the joint/link number. It should be mentioned that the nominal DH parameters d_1, d_6 and the joint offsets $\Delta q_1, \Delta q_6$ cannot be identified separately from the base or tool transformations (they are semi-identifiable in the complete model), so they have been eliminated from the set of principal parameters.

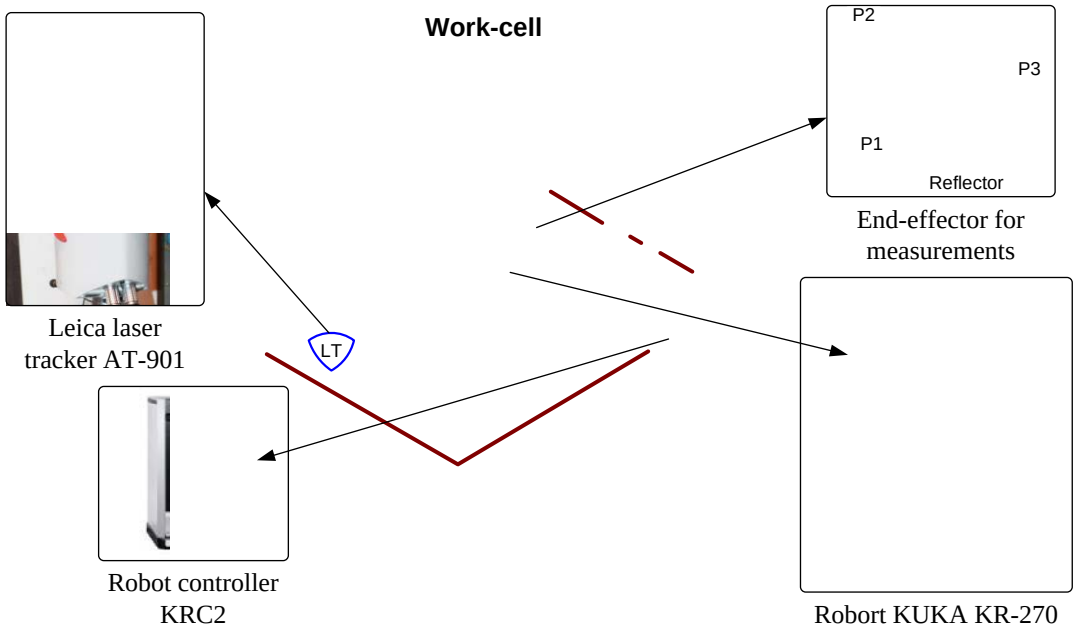

Figure 8 Experimental setup for geometric calibration

To get the desired measurement data, the robotic cell was equipped with a Laser tracker Leica AT-901 that provided us with Cartesian coordinates of three references points. The manipulator joint angles required for the identification procedure were obtained from the robot controler. The experimental setup for manipulator geometric calibration is presented in Figure 8.

To reduce the influence of the non-geometric factors, the measurements were repeated three times for each configuration. As a result, the measurement data of each manipulator configuration contain 27 position coordinates. It is worth mentioning that the whole data set contains 432 coordinates $\{p_{xi}, p_{yi}, p_{zi}\}$. Using the obtained data, the identification procedure was applied. The identification results are given in Table 9. It should be stressed that some of these parameters cannot be modified in the robot control software. So, it is reasonable to examine the effect of reducing the number of these parameters by setting them to their nominal values. For this purposes, the *parameter-to-noise ratios* were computed (here, the estimated value of the noise parameter σ is about 0.1 mm.). The results show that for the parameters $\varphi_{z3}, \Delta q_4, p_{z4}, \Delta q_5, p_{z5}, \varphi_{z5}$ this indicator is extremely low, i.e. their identification accuracy is not high enough to distinguish the identified value from zero. Therefore, it is reasonable to eliminate them from the model.

Table 9 Identification results for geometric calibration for industrial robot Kuka KR-270 (*full model*)

Parameter	Unit .	Nominal value	Identified deviation	Confidence interval	Parameter-to-noise ratio	Subset
$p_{x1} \equiv \Delta d_2$	[mm]	350.0	-0.334	±0.086	11.7	G1+
p_{y1}	[mm]	0	0.571	±0.272	6.3	G1+
φ_{x1}	[deg]	0	0.018	±0.005	12.0	G1+
Δq_2	[deg]	0	-0.008	±0.005	5.1	G1~
$p_{x2} \equiv \Delta d_3$	[mm]	1250.0	0.456	±0.082	16.7	G1+
φ_{x2}	[deg]	0	0.020	±0.014	4.3	G1~
φ_{z2}	[deg]	0	-0.021	±0.005	13.5	G1+
Δq_3	[deg]	0	-0.025	±0.019	4.0	G1~
$p_{x3} \equiv \Delta d_4$	[mm]	1100.0	-0.229	±0.089	7.7	G1+
$p_{z3} \equiv \Delta d_5$	[mm]	-55.0	-0.534	±0.363	4.4	G1~
φ_{z3}	[deg]	0	-0.007	±0.017	1.3	G1-
Δq_4	[deg]	0	0.001	±0.008	0.3	G1-
p_{y4}	[mm]	0	-0.151	±0.113	4.0	G1~
p_{z4}	[mm]	0	-0.027	±0.073	1.1	G1-
φ_{z4}	[deg]	0	0.026	±0.015	5.1	G1~
Δq_5	[deg]	0	-0.011	±0.027	1.3	G1-
p_{z5}	[mm]	0	0.007	±0.104	0.2	G1-
φ_{z5}	[deg]	0	-0.010	±0.018	1.6	G1-

For comparison purposes, the manipulator accuracy improvement due to calibration has been studied based on the residual analysis before and after calibration. Here, two types of residuals have been examined, the coordinate-based and distance-based ones. Corresponding results are presented in Table 10, which includes the maximum and root mean square (RMS) values of the relevant residuals. As follows from the results, the residuals were essentially reduced after calibration both for full and reduced models. In particular, the maximum values have been reduced by a factor of 3.5-4.2, while the RMS values of these two criteria have been decreased by a factor of 4.9-5.3. Moreover, maximum errors have been slightly decreased in the reduced model

comparing with the full one. Hence, the obtained results confirm the reduced model suitability for the geometric errors compensation.

Table 10 Manipulator accuracy improvement after geometric calibration.

Criterion		Residuals, [mm]			
		Coordinate-based		Distance-based	
		max	RMS	max	RMS
Accuracy before calibration		1.25	0.54	1.31	0.94
Accuracy after calibration	Full model	0.32	0.10	0.37	0.18
	Reduced model A*	0.30	0.11	0.36	0.19
	Reduced model B**	0.32	0.10	0.37	0.18
Improvement factor	Full model	4.0	5.3	3.5	5.2
	Reduced model A*	4.2	4.9	3.6	4.9
	Reduced model B**	4.0	5.3	3.5	5.2

* Parameers have been identified using full model (18 parameter, condition number equal 60.6)

** Parameers have been identified using reduced model (12 parameters, condition number equal 29.7)

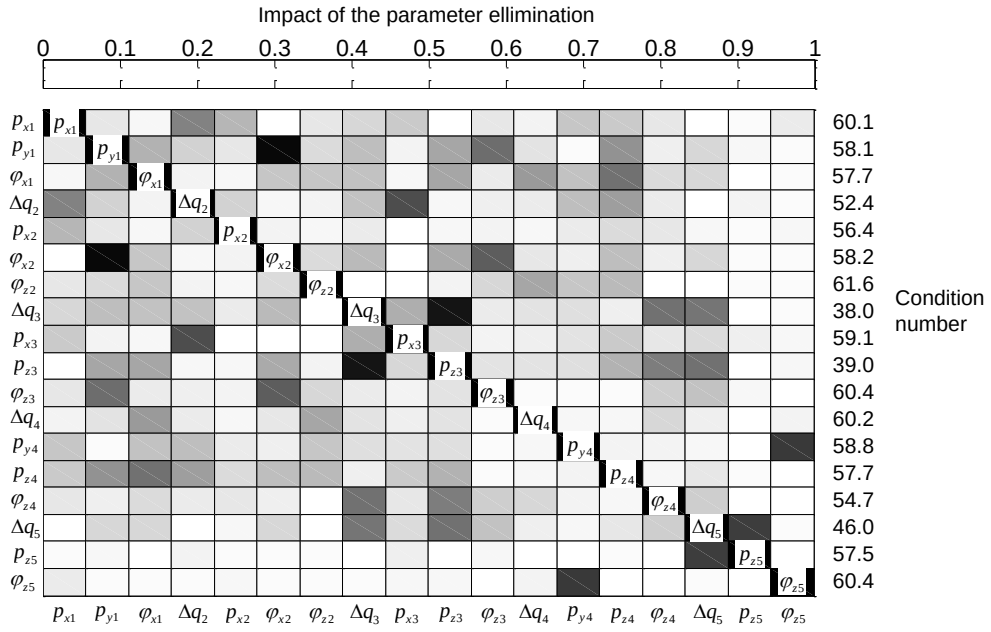

Figure 9 Empirical elimination of small parameters and its impact on the identification results.

In order to verify the reduced model validity from another point of view, the impact of a single parameter elimination (for the whole set) has been evaluated. Relevant results are presented in Figure 9, which contains a table showing how much parameter-to-noise ratio changes if *i*-th parameter is eliminated from the model. The *i*-th line of the table corresponds to the reduced model that does not include the *i*-th parameter only. The remaining elements of the line show the sensitivity of rest of the parameters to this elimination. The sensitivity is normalized with respect to parameter deviations (σ_i) that make them equivalent to the change of the parameter-to-noise ratio ν_i. In fact, if the off-diagonal values are less than 3, the deviations in corresponding parameters will be inside of the confidence interval with the probability 99.8%. On the right-hand side of the table, the condition numbers of the corresponding (reduced) observation matrices are provided. It should be noted that the condition number of the original observation matrix is equal to 60.7. The presented results show that whatever parameter is eliminated, the identified values of the remaining parameters are almost the same. That means that the reduced model is practically acceptable for the calibration.

Table 11 Identification results for geometric calibration for industrial robot Kuka KR-270 (*reduced model*)

Parameter	Unit.	Identified deviation		Potential loss of accuracy, [mm]	Confidence interval	Parameter-to-noise ratio	
		Full model	Reduced model			Full model	Reduced model
p_{x1}	[mm]	-0.334	-0.321	0.013	±0.083	11.7	11.6
p_{y1}	[mm]	0.571	0.526	0.045	±0.150	6.3	10.5
φ_{x1}	[deg]	0.018	0.017	0.010	±0.003	12.0	15.0
Δq_2	[deg]	-0.008	-0.008	0.022	±0.004	5.1	6.1
p_{x2}	[mm]	0.456	0.448	0.008	±0.080	16.7	16.7
φ_{x2}	[deg]	0.020	0.021	0.025	±0.008	4.3	8.3
φ_{z2}	[deg]	-0.021	-0.021	0.024	±0.004	13.5	15.7
Δq_3	[deg]	-0.025	-0.035	0.203	±0.009	4.0	11.2
p_{x3}	[mm]	-0.229	-0.234	0.005	±0.084	7.7	8.2
p_{z3}	[mm]	-0.534	-0.764	0.230	±0.167	4.4	13.8
p_{y4}	[mm]	-0.151	-0.201	0.050	±0.070	4.0	8.6
φ_{z4}	[deg]	0.026	0.028	0.005	±0.013	5.1	6.2

Hence, for the considered problem, it is prudent to use the reduced geometric model that does not include the following parameters: $\varphi_{z3}, \Delta q_4, p_{z4}, \Delta q_5, p_{z5}, \varphi_{z5}$. The validity of the reduced model for the compensation has been confirmed by the residual analysis. As follows from Table 10, the residuals do not change significantly because of the parameters elimination. Besides, the elimination leads to the improvement of the observation matrix condition number (it has been reduced from 60.6 to 29.7). Corresponding identification results as well as potential lose of the robot positioning accuracy caused by the model reduction are summarized in Table 11. In spite of the fact that for some parameters (such as Δq_3, p_{z3}) potential loss of the accuracy is more than 0.2 mm. So, the reduced model insures almost the same compensation capacity as the complete one (see Table 10). Therefore, the experimental study presented in this Section, which illustrates the application of developed theoretical results, confirms benefits of the developed approach.

7 Conclusions

The paper deals with the problem of the manipulator stiffness modeling, which is extremely important for the robotic-based machining of contemporary aeronautic materials where high position accuracy is required while performing prescribed manufacturing task. The main attention is paid to the elastostatic parameters identification and model reduction, where the notion of practical identifiability is introduced that relies on the essential differences in the model parameter magnitudes and the measurement noise impact.

In contrast to previous works, the manipulator stiffness properties are described by the sophisticated model, which takes into account the flexibilities of all mechanical elements such as links, actuated joints, mechanical transmissions, etc. In the frame of this model, the virtual joint method (VJM) is used, which operates with 6×6 stiffness matrices for each compliant link and scalar coefficients for the joints/transmissions. This yields extremely high number of the model elastostatic parameters to be identified, that for a conventional 6 d.o.f. manipulator reaches 258. Even by eliminating dependent ones does not allow us to reduce this number substantially; for a typical manipulator the stiffness model includes 153 independent parameters that, theoretically, may be identified. However, the parameter magnitudes differ significantly (~1000 times), so straightforward application of conventional identification technique does not give reliable results (for some parameters the estimation errors are greater than 100% that also may violate fundamental physical properties of the stiffness matrices, such as *positive-definiteness and symmetry*). On the other hand, some of the desired parameters are so small that their influence on the manipulator accuracy is negligible. This leads the problem of further reduction of the stiffness model that aims at eliminating some small parameters. To distinguish these small parameters from essential ones, the notion of practical identifiability was introduced.

To solve the problem, physical, algebraical and statistical model reduction methods were developed. They take into account mathematical relations between the elements of the compliance matrices and parameter magnitude with respect to the measurement noise impact. In spite of the fact that main theoretical results have been developed for elastostatic calibration, they can be also efficiently applied for geometric case. The advantages of the developed approach are illustrated by two application examples that deal with elastostatic and geometric calibration of industrial robot used in aerospace industry in real industrial environment. In future, the problem of the complete model reconstruction from the obtained set of practically identifiable parameters will be in the focus of our attention.

8 Acknowledgments

The work presented in this paper was partially funded by the Region “Pays de la Loire”, France and by the projects ANR COROUSSO and FEDER ROBOTEX, France.

9 References

[1] P. Dépincé, J.-Y. Hascoët, Active integration of tool deflection effects in end milling. Part 1. Prediction of milled surfaces, International Journal of Machine Tools and Manufacture, 46 (2006) 937-944.

[2] S.J. Eastwood, P. Webb, A gravitational deflection compensation strategy for HPKMs, Robotics and Computer-Integrated Manufacturing, 26 (2010) 694-702.

[3] J. Kövecses, J. Angeles, The stiffness matrix in elastically articulated rigid-body systems, Multibody System Dynamics, 18 (2007) 169-184.

[4] A. Klimchik, D. Bondarenko, A. Pashkevich, S. Briot, B. Furet, Compliance Error Compensation in Robotic-Based Milling, in: J.-L. Ferrier, A. Bernard, O. Gusikhin, K. Madani (Eds.) Informatics in Control, Automation and Robotics, Springer International Publishing, 2014, pp. 197-216.

[5] B. Karan, M. Vukobratović, Calibration and accuracy of manipulation robot models—An overview, Mechanism and Machine Theory, 29 (1994) 479-500.

[6] E. Abele, K. Schützer, J. Bauer, M. Pischan, Tool path adaption based on optical measurement data for milling with industrial robots, Prod. Eng. Res. Devel., 6 (2012) 459-465.

[7] Y. Chen, J. Gao, H. Deng, D. Zheng, X. Chen, R. Kelly, Spatial statistical analysis and compensation of machining errors for complex surfaces, Precision Engineering, 37 (2013) 203-212.

[8] C.-C. Lo, C.-Y. Hsiao, A method of tool path compensation for repeated machining process, International Journal of Machine Tools and Manufacture, 38 (1998) 205-213.

[9] L.J. Everett, T.-W. Hsu, The theory of kinematic parameter identification for industrial robots, J. DYN. SYST. MEAS. CONTROL., 110 (1988) 96-100.

[10] B.W. Mooring, Z.S. Roth, M.R. Driels, Fundamentals of manipulator calibration, Wiley New York, 1991.

[11] A. De Luca, B. Siciliano, L. Zollo, PD control with on-line gravity compensation for robots with elastic joints: Theory and experiments, Automatica, 41 (2005) 1809-1819.

[12] T.-f. Lu, G.C.I. Lin, An on-line relative position and orientation error calibration methodology for workcell robot operations, Robotics and Computer-Integrated Manufacturing, 13 (1997) 89-99.

[13] A. Klimchik, A. Pashkevich, D. Chablat, G. Hovland, Compliance error compensation technique for parallel robots composed of non-perfect serial chains, Robotics and Computer-Integrated Manufacturing, 29 (2013) 385-393.

[14] J.H. Jang, S.H. Kim, Y.K. Kwak, Calibration of geometric and non-geometric errors of an industrial robot, Robotica, 19 (2001) 311-321.

[15] M.A. Meggiolaro, S. Dubowsky, C. Mavroidis, Geometric and elastic error calibration of a high accuracy patient positioning system, Mechanism and Machine Theory, 40 (2005) 415-427.

[16] Z.S. Roth, B. Mooring, B. Ravani, An overview of robot calibration, Robotics and Automation, IEEE Journal of, 3 (1987) 377-385.

[17] J.M. Hollerbach, A survey of kinematic calibration, The robotics review 1, MIT Press, 1989, pp. 207-242.

[18] W. Veitschegger, C.H. Wu, A method for calibrating and compensating robot kinematic errors, Robotics and Automation. Proceedings. 1987 IEEE International Conference on, 1987, pp. 39-44.

[19] J. Hollerbach, W. Khalil, M. Gautier, Model Identification, in: B. Siciliano, O. Khatib (Eds.) Springer Handbook of Robotics, Springer Berlin Heidelberg, 2008, pp. 321-344.

[20] S.A. Hayati, Robot arm geometric link parameter estimation, Decision and Control, 1983. The 22nd IEEE Conference on, IEEE, 1983, pp. 1477-1483.

[21] S. Hayati, K. Tso, G. Roston, Robot geometry calibration, Robotics and Automation, 1988. Proceedings., 1988 IEEE International Conference on, 1988, pp. 947-951 vol.942.

[22] H.W. Stone, Kinematic modeling, identification, and control of robotic manipulators, Springer, 1987.

[23] D.E. Whitney, C.A. Lozinski, J.M. Rourke, Industrial Robot Forward Calibration Method and Results, Journal of Dynamic Systems, Measurement, and Control, 108 (1986) 1-8.

[24] I.M. Chen, G. Yang, C.T. Tan, S.H. Yeo, Local POE model for robot kinematic calibration, Mechanism and Machine Theory, 36 (2001) 1215-1239.

[25] X. Yang, L. Wu, J. Li, K. Chen, A minimal kinematic model for serial robot calibration using POE formula, Robotics and Computer-Integrated Manufacturing, 30 (2014) 326-334.

[26] G. Piras, W.L. Cleghorn, J.K. Mills, Dynamic finite-element analysis of a planar high-speed, high-precision parallel manipulator with flexible links, Mechanism and Machine Theory, 40 (2005) 849-862.

[27] C.S. Long, J.A. Snyman, A.A. Groenwold, Optimal structural design of a planar parallel platform for machining, Applied Mathematical Modelling, 27 (2003) 581-609.

[28] D. Deblaise, X. Hernot, P. Maurine, A systematic analytical method for PKM stiffness matrix calculation, Robotics and Automation, 2006. ICRA 2006. Proceedings 2006 IEEE International Conference on, IEEE, 2006, pp. 4213-4219.

[29] G. Alici, B. Shirinzadeh, Enhanced stiffness modeling, identification and characterization for robot manipulators, Robotics, IEEE Transactions on, 21 (2005) 554-564.

[30] S.-F. Chen, I. Kao, Conservative congruence transformation for joint and Cartesian stiffness matrices of robotic hands and fingers, The International Journal of Robotics Research, 19 (2000) 835-847.

[31] A. Pashkevich, D. Chablat, P. Wenger, Stiffness analysis of overconstrained parallel manipulators, Mechanism and Machine Theory, 44 (2009) 966-982.

[32] C. Quennouelle, C.á. Gosselin, Stiffness matrix of compliant parallel mechanisms, Advances in Robot Kinematics: Analysis and Design, Springer, 2008, pp. 331-341.

[33] A. Nubiola, I.A. Bonev, Absolute calibration of an ABB IRB 1600 robot using a laser tracker, Robotics and Computer-Integrated Manufacturing, 29 (2013) 236-245.

[34] B. Ying, Z. Hanqi, Z.S. Roth, Experiment study of PUMA robot calibration using a laser tracking system, Soft Computing in Industrial Applications, 2003. SMCia/03. Proceedings of the 2003 IEEE International Workshop on, 2003, pp. 139-144.

[35] A. Klimchik, Y. Wu, C. Dumas, S. Caro, B. Furet, A. Pashkevich, Identification of geometrical and elastostatic parameters of heavy industrial robots, Robotics and Automation (ICRA), 2013 IEEE International Conference on, 2013, pp. 3707-3714.

[36] Y. Takeda, G. Shen, H. Funabashi, A DBB-based kinematic calibration method for in-parallel actuated mechanisms using a Fourier series, Journal of Mechanical Design, 126 (2004) 856.

[37] M. Ikits, J.M. Hollerbach, Kinematic calibration using a plane constraint, Robotics and Automation, 1997. Proceedings., 1997 IEEE International Conference on, IEEE, 1997, pp. 3191-3196.

[38] L. Beyer, J. Wulfsberg, Practical robot calibration with ROSY, Robotica, 22 (2004) 505-512.

[39] Y. Liu, Z. Jiang, H. Liu, W. Xu, Geometric Parameter Identification of a 6-DOF Space Robot Using a Laser-Ranger, Journal of Robotics, 2012 (2012).

[40] I. Park, B. Lee, S. Cho, Y. Hong, J. Kim, Laser-based kinematic calibration of robot manipulator using differential kinematics, Mechatronics, IEEE/ASME Transactions on, 17 (2012) 1059-1067.

[41] J. Liu, Y. Zhang, Z. Li, Improving the positioning accuracy of a neurosurgical robot system, Mechatronics, IEEE/ASME Transactions on, 12 (2007) 527-533.

[42] J. Santolaria, J.-J. Aguilar, J.-A. Yagüe, J. Pastor, Kinematic parameter estimation technique for calibration and repeatability improvement of articulated arm coordinate measuring machines, Precision Engineering, 32 (2008) 251-268.

[43] C. Lightcap, S. Hamner, T. Schmitz, S. Banks, Improved positioning accuracy of the PA10-6CE robot with geometric and flexibility calibration, Robotics, IEEE Transactions on, 24 (2008) 452-456.

[44] J. Santolaria, J. Conte, M. Ginés, Laser tracker-based kinematic parameter calibration of industrial robots by improved CPA method and active retroreflector, The International Journal of Advanced Manufacturing Technology, (2013) 1-20.

[45] I. Williams, G. Hovland, T. Brogardh, Kinematic error calibration of the gantry-tau parallel manipulator, Robotics and Automation, 2006. ICRA 2006. Proceedings 2006 IEEE International Conference on, IEEE, 2006, pp. 4199-4204.

[46] C. Gong, J. Yuan, J. Ni, Nongeometric error identification and compensation for robotic system by inverse calibration, International Journal of Machine Tools and Manufacture, 40 (2000) 2119-2137.

[47] J.-H. Borm, C.-H. Menq, Determination of Optimal Measurement Configurations for Robot Calibration Based on Observability Measure, The International Journal of Robotics Research, 10 (1991) 51-63.

[48] A.C. Atkinson, A.N. Donev, Optimum Experimental Designs, volume 8 of Oxford Statistical Science Series, Oxford University Press, Oxford, UK, 1992.

[49] Z. Hanqi, L. Lixin, Self-calibration of a class of parallel manipulators, Robotics and Automation, 1996. Proceedings., 1996 IEEE International Conference on, 1996, pp. 994-999 vol.992.

[50] W. Khalil, S. Besnard, Self calibration of Stewart-Gough parallel robots without extra sensors, Robotics and Automation, IEEE Transactions on, 15 (1999) 1116-1121.

[51] W. Khalil, M. Gautier, C. Enguehard, Identifiable parameters and optimum configurations for robots calibration, Robotica, 9 (1991) 63-70.

[52] A. Nahvi, J.M. Hollerbach, The noise amplification index for optimal pose selection in robot calibration, Robotics and Automation, 1996. Proceedings., 1996 IEEE International Conference on, IEEE, 1996, pp. 647-654.

[53] D. Daney, Optimal measurement configurations for Gough platform calibration, Robotics and Automation, 2002. Proceedings. ICRA'02. IEEE International Conference on, IEEE, 2002, pp. 147-152.

[54] A. Klimchik, Y. Wu, S. Caro, A. Pashkevich, Design of experiments for calibration of planar anthropomorphic manipulators, Advanced Intelligent Mechatronics (AIM), 2011 IEEE/ASME International Conference on, IEEE, 2011, pp. 576-581.

[55] H. Zhuang, K. Wang, Z.S. Roth, Optimal selection of measurement configurations for robot calibration using simulated annealing, Robotics and Automation, 1994. Proceedings., 1994 IEEE International Conference on, IEEE, 1994, pp. 393-398.

[56] J. Imoto, Y. Takeda, H. Saito, K. Ichiryu, Optimal kinematic calibration of robots based on maximum positioning-error estimation (Theory and application to a parallel-mechanism pipe bender), Computational Kinematics, Springer, 2009, pp. 133-140.

[57] A. Klimchik, Y. Wu, A. Pashkevich, S. Caro, B. Furet, Optimal Selection of Measurement Configurations for Stiffness Model Calibration of Anthropomorphic Manipulators, Applied Mechanics and Materials, 162 (2012) 161-170.

[58] W. Jianjun, Z. Hui, T. Fuhlbrigge, Improving machining accuracy with robot deformation compensation, IEEE/RSJ International Conference on Intelligent Robots and Systems (IROS 2009). , 2009, pp. 3826-3831.

[59] C. Dumas, S. Caro, S. Garnier, B. Furet, Joint stiffness identification of six-revolute industrial serial robots, Robotics and Computer-Integrated Manufacturing, 27 (2011) 881-888.

[60] A. Klimchik, A. Pashkevich, D. Chablat, CAD-based approach for identification of elasto-static parameters of robotic manipulators, Finite Elements in Analysis and Design, 75 (2013) 19-30.

[61] L. Everett, M. Driels, B.W. Mooring, Kinematic modelling for robot calibration, Robotics and Automation. Proceedings. 1987 IEEE International Conference on, 1987, pp. 183-189.

[62] W. Khalil, E. Dombre, Modeling, identification and control of robots, Butterworth-Heinemann, 2004.

[63] A. Pashkevich, Computer-aided generation of complete irreducible models for robotic manipulators, The 3rd Int. Conference of Modellimg and Simulation. University of Technology of Troyes, France, 2001, pp. 293-298.

[64] A. Pashkevich, A. Klimchik, D. Chablat, Enhanced stiffness modeling of manipulators with passive joints, Mechanism and machine theory, 46 (2011) 662-679.

[65] A. Klimchik, D. Chablat, A. Pashkevich, Stiffness modeling for perfect and non-perfect parallel manipulators under internal and external loadings, Mechanism and Machine Theory, 79 (2014) 1-28.

[66] J. Angeles, Fundamentals of robotic mechanical systems: theory, methods, and algorithms, Springer, 2007.

[67] J. Rice, Mathematical statistics and data analysis, Cengage Learning, 2006.

[68] D. Daney, Y. Papegay, B. Madeline, Choosing measurement poses for robot calibration with the local convergence method and Tabu search, The International Journal of Robotics Research, 24 (2005) 501-518.

[69] S. Timoshenko, J.N. Goodier, Theory of elasticity, 3rd ed. ed., McGraw-Hill, Singapore 1970.